Accepted Manuscript

Shrimp zircon geochronology constrains on Permian pyroclastic levels, Claromecó Basin, South West margin of Gondwana, Argentina

Guadalupe Arzadún, Renata N. Tomezzoli, Ricardo Trindade, Leandro C. Gallo, Nora N. Cesaretti, Juan M. Calvagno

PII: S0895-9811(17)30449-2

DOI: 10.1016/j.jsames.2018.05.001

Reference: SAMES 1923

To appear in: *Journal of South American Earth Sciences*

Received Date: 6 November 2017

Revised Date: 24 April 2018

Accepted Date: 1 May 2018

Please cite this article as: Arzadún, G., Tomezzoli, R.N., Trindade, R., Gallo, L.C., Cesaretti, N.N., Calvagno, J.M., Shrimp zircon geochronology constrains on Permian pyroclastic levels, Claromecó Basin, South West margin of Gondwana, Argentina, *Journal of South American Earth Sciences* (2018), doi: 10.1016/j.jsames.2018.05.001.

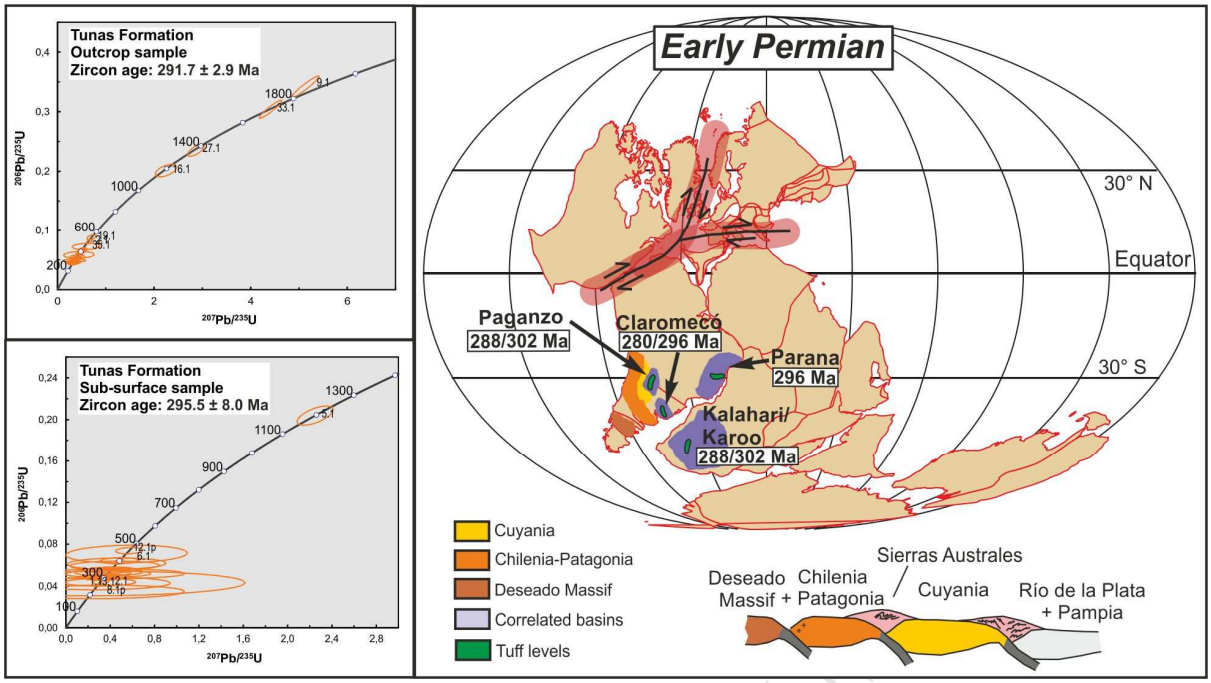

SHRIMP ZIRCON GEOCHRONOLOGY CONSTRAINS ON PERMIAN PYROCLASTIC LEVELS, CLAROMECÓ BASIN, SOUTH WEST MARGIN OF GONDWANA, ARGENTINA

Guadalupe Arzadún[1,2], Renata N. Tomezzoli[1,3], Ricardo Trindade[4], Leandro C. Gallo[1,3], Nora N. Cesaretti[5], Juan M. Calvagno[1,3]

[1]Consejo Nacional de Investigaciones Científicas y Técnicas (CONICET). E-mail: guadalupe.arzadun@gmail.com,

[2] La.Te. Andes. Laboratorio de Termocronología. Las Moreras 310, Vaqueros, Salta.

[3]IGEBA. Instituto de Geociencias Básicas y Aplicadas de Buenos Aires. Laboratorio de Paleomagnetismo D.A. Valencio. Departamento de Geología, Facultad de Ciencias Exactas y Naturales. Universidad de Buenos Aires.

[4]Instituto de Astronomia, Geofísica e Ciências Atmosféricas, Universidade de São Paulo, São Paulo, Brazil.

[5]Depto de Geología, UNS, Bahía Blanca, Argentina Departamento de Geología, Universidad Nacional del Sur, Bahía Blanca, Argentina

Abstract. Pyroclastic levels are descripted in Sierras Australes outcrops and Claromeco Basin sub-surface records, interbedded with mudrocks and coal beds in the base of the Tunas Formation sequence that correspond to the Permian South West margin of Gondwana. The pyroclastic levels classify as fine tuff. SHRIMP zircon ages obtained are 291.7 ± 2.9 Ma in the outcrop and 295.5 ± 8.0 Ma in the subsurface. These ages are consistent with other zircon SHRIMP ages of other outcrops tuff of the Tunas Formation, with Permian flora, and with tuff ages of correlated Gondwana areas, in the Paraná, Karoo and Paganzo basins. These data, in addition with other geological evidences, support a tectonically active and changing

environment during the Permian of Gondwana. The ages allowed calculating a northward latitudinal speed of 2.7 cm/year for Gondwana during the Permian. This latitudinal movement is explained as the consequence of the final coupling of several continental microplates, gradually amalgamated from the southern margins of Gondwana and from the northern of Laurentia to configure the final Pangea during the Triassic. Since the main accretions in the southwestern margin of Gondwana could have started during the Devonian - Carboniferous, this Permian orogeny (San Rafael Orogenic Phase in Argentina) would be representing the post - collisional deformation, with a peak of compression in the Early Permian that was attenuating towards the foreland during the Late Permian - Early Triassic. With these results, it is also possible to constraint the age of the upper Paleozoic glaciation up to 295, previous to the deposition of the Tunas Formation in the Sauce Grande Formation.

Introduction

The Sierras Australes Bonaerenses, also known as Sierra de la Ventana or Ventania system, are located between the 37° and 39° South Latitude and 61° and 63° West Longitude, in the Buenos Aires province, Argentina. They are the outcrop portion of the Claromecó Basin (Kostadinoff and Prozzi, 1998; Ramos, 1984; Lesta and Sylwan, 2005; Pángaro and Ramos, 2012; Figure 1) that developed on the southwest margin of the Gondwana continent during the Paleozoic (Figure 1, Keidel, 1916; Harrington, 1947; Suero, 1972; Kilmurray, 1975), and are considered the South American counterpart of the Cape Fold Belt in South Africa (Du Toit, 1927; Zambrano, 1974). Recently, this sector was interpreted as part of the Hesperides Basin, laterally integrated with the Kalahari, Karoo and Chaco-Paraná Basins in Africa and South America, with a depocenter of more than 3000000 Km^2 that was active during the Late Carboniferous and Early Triassic (Pángaro *et al.*, 2015).

The outcrops of the Sierras Australes have a general northwest-southeast trend. Their ages range from the Late Precambrian to the Permian, with the oldest rocks outcropping at the west and the most modern ones at the east. Cenozoic deposits cover unconformable these units (Figure 1). Ramos (1984), Von Gosen *et al.* (1991), and Tomezzoli and Cristallini (1998, 2004) consider the Sierras Australes as a thrust and fold belt. The vergence of the system is northeastern, decreasing the intensity of the deformation from west to east (Harrington, 1947; Tomezzoli, 2001; Arzadún *et al.*, 2016) (Figure 2).

The structure of the Sierras Australes was initially interpreted as a system deformed dominantly by folding (Harrington, 1947). Ramos (1984), Chernicoff *et al.* (2013) and Ramos *et al.* (2013) assumed that the Sierras Australes structure is the product of an intercontinental collision between Patagonia and Gondwana during the Late Paleozoic, and the Claromecó Basin represents the foreland basin. Other authors suggest a system of continental blocks, which move due a tectonic event producing crustal fragmentation through transformed faults (Kostadinoff, 1993; Álvarez, 2004; Kostadinoff, 2007; Gregori *et al.*, 2003, 2008). Rapallini, (2005) and Rapallini *et al.* (2013), suggest a para-authochtonous origin of Patagonia. Some contributions analyzed the structures at different scales and its evolution has been interpreted through various tectonic models. Rossello and Massabie (1981) suggested a coaxial deformation model and interpreted the structures as the result of a non-rotational pure shear deformation. Other authors assumed a non-coaxial deformation model, with conditions of deformation dominated by simple shear (Cobbold *et al.*, 1987, 1991; Japas, 1995a, 1995b, 1999; Rossello and Massabie, 1992; von Gosen *et al.*, 1990). Tomezzoli (2012) suggests that the deformation is a combination of the different processes that occurs from the Late Devonian and continuous until the Permian.

The Pillahuincó Group (Harrington, 1947; Lesta and Sylwan, 2005) correspond to the sedimentary succession of the Late Carboniferous to Late Permian, situated in the Sierras

Australes and in the Claromecó Basin. Four formations integrate this group, called from the base to the top, Sauce Grande, Piedra Azul, Bonete and Tunas (Figure 1b; Harrington, 1972). In this work, new pyroclastic levels are reported in the Tunas Formation sequence, from outcrops intercalated in the base and from subsurface. The outcrops are in the Ruta 76 locality, and the core records belong to the PANG0001 well are in the Claromecó Basin (Figure 1). In these levels, new radiometric ages were obtained by U-Pb SHRIMP analyses on zircon crystal, which contribute to understanding their regional significance and brings out new information to shed light in the complex correlation of Carboniferous-Permian basins across the southwestern margin of Gondwana. During this time, the Late Paleozoic Ice Age (LPIA) occurs, one of the Earth's most important climatic events as represent the longest and most widespread glacial interval. However, the distribution, timing and size of its events remains unsolved (Fielding *et al.*, 2008; Isbell *et al.*, 2003; Frank *et al.*, 2015). The understanding of the LPIA largely depends on the increasing precision of Permo-Carboniferous chronostratigraphy (Montañez and Poulsen, 2013). With these results is also possible to constraint the maximum age of the Late Paleozoic glaciation.

Geological setting

The Pillahuincó Group outcrops at the east of the Sierras Australes, and continue at subsurface in the Claromecó Basin (Figure 1b). The Sauce Grande Formation (Harrington, 1947) that is the base of the Pillahuincó Group, has 1100 m of diamictite deposits, sandstones and in minor proportion mudrocks (Andreis *et al.*, 1989). Coates (1969), Harrington (1980), Andreis (1984) interpreted these diamictites as glaci-marine deposits. The palinological contain indicate a Pennsylvanian-Cisuralian age (Di Pasquo *et al.*, 2008). In the diamictitic section of the Puelches well, situated in the Claromecó Basin, has be found spores that suggest a late Carboniferous to early Permian age (Archangelsky *et al.*, 1987). In transitional

contact, is the Piedra Azul Formation with 300 m of mudrocks, heterolites and minor fine sandstones (Harrington, 1947; Japas, 1986). It correspond to a marine environment when the glacial conditions finished (López Gamundi, 1989; Andreis and Japas, 1996).

The Bonete Formation (Harrington, 1947) is in concordance above the Piedra Azul Formation. It has 400 m of fine-grain arkosic sandstones of green color, with whitish specks, intercalated with dark gray mudrocks. The sandstones have abundant remains of marine invertebrates belonging to the "*Eurydesma* faune" (Harrington, 1955; Rocha Campos and Carvalho, 1975; Amos, 1980). Archangelsky and Cúneo (1984) found remains of plants that belong to the *Glossopteris* Zone. The fossils indicate an early Permian age.

The Tunas Formation outcrops in the northeast portion of the Sierras Australes, from the north in the Sierra de Las Tunas to the south in the Sierra de Pillahuincó and continues eastwards in sub-surface in the Claromecó Basin (Ramos, 1984; Tomezzoli and Vilas, 1997; Kostadinoff and Prozzi, 1998; Lesta and Sylwan, 2005; Pángaro and Ramos, 2012; Figures 1a and 1b). Several authors described small outcrops near the González Chávez locality, situated at the east, into the Claromecó Basin area, with fossil plants assignable to the Upper Paleozoic, similar to those recognized in the Sierras Australes (Figure 1, Monteverde, 1937; Amos and Urien, 1968; Zambrano, 1974; Llambías and Prozzi, 1975; Kostadinoff and Font, 1982). It has fine-grain to medium-grain sandstones of green, gray, red and yellow colors, with cross stratification, intercalate with siltstones of red and green colors (Andreis *et al.*, 1979; Andreis and Cladera, 1992; López Gamundi, 1996).

The siltstones have plants remain of *Glossopteris* and lycopsids, and poor preserved bivalve remains (Harrington, 1947; Furque, 1973; Ruiz and Bianco, 1985). The *Glossopteris* flora suggests ages from the Sakmarian to the Artinskian (Harrington, 1947; Furque, 1973; Andreis *et al*., 1979; Ruiz and Bianco, 1985; López Gamundi, 1996; Archangelsky and Cúneo, 1984). Falco and Arzadún (2012) describe deformation structures that consist in pseunodules and

flame structures in the upper section of the Tunas Formation and relate them to seismic events occurring at the time of sedimentation.

Iñiguez *et al.* (1988) described pyroclastic levels at the Abra del Despeñadero, at the east of Sierras Australes, on Ruta 51 (Figure 1b), at the upper section of the Tunas Formation (Harrington, 1947). The petrographic analysis performed by these authors indicates the presence of clay minerals such as beidellite, illite and vermiculite. They consider that beidellite is a product of the alteration of vitreous materials of pyroclastic origin, accumulated in an aqueous environment from the fall of tefra. López-Gamundi *et al.* (2013) obtain SHRIMP ages of 280.8 ± 1.9 Ma for these levels, and suggest that the volcanism in the Sierras Australes and Claromecó Basin is the distal equivalent of the precursory Choiyoi magmatic province, which extension exceeds 500,000 km^2 and covers practically all the west of Argentina during the Permian–Triassic time (Llambías *et al.*, 2003).

There are several discrepancies about the Tunas Formation thickness. Andreis *et al.* (1979) measured an outcropping thickness of 710 m in the west, while Suero (1975) mentions 2400 m in the southeast sector and Japas (1986) measured 1000 m in outcrop. Zorzano *et al.* (2011) mention an outcropping thickness of 1000 m for this formation and a thickness of more than 960 m in subsurface, not recognizing its base. Lesta and Sylwan (2005) estimated 600 m in the "Ventania" sector and more than 600 m in subsurface based on seismic data and drilling.

Andreis *et al.* (1989) interpreted the base of the Tunas Formation as the culmination of the regressive cycle, after shallow marine conditions of the Bonete Formation. Zavala *et al.* (1993) reported the presence of fluvial deposits at Las Mostazas, located towards the top of the outcropping sequence of the Sierras Australes (Figure 1b). Zorzano *et al.* (2011) describe shale facies belonging to a platform and prodelta environment, sandy platform lobes related to wave dominated platform bars and river-banks and estuarine fluvial channels, interdistributaries swamp corresponding to alluvial plain.

In base to compositional considerations of Lopez Gamundi (1996), the Sauce Grande, Piedra Azul and Bonete Formations share a common cratonic origin and a sedimentary evolution integrated by glacimarine conditions (Sauce Grande Formation) followed by a transgression, represented by open platform sedimentation (Piedra Azul and Bonete Formations). On the other hand, for the Tunas Formation, different areas of provenance are inferred, evidenced by changes in the detrital modes characterized by low to moderate percentages of quartz and abundant lithic fragments of volcanic and metamorphic origin.

These lithological changes would be related to the tectonic events that would have affected the southwestern margin of the basin during those times.

The presence of red strata is attributed to the oxidized ferruginous compounds, mainly hematite of primary origin that suggests a quickly input of sediments rapidly covered by other detrital material (Andreis *et al.*, 1979).

Anisotropy of magnetic susceptibility (AMS) data in the Tunas Formation indicate a decrease in the deformation towards the east. Also, indicate a stress from the SW that attenuated from the Early to Late Permian, evidencing the migration of the orogenic front to the foreland basin located towards the northeast (Arzadún *et al.*, 2016; Figure 1). The differences in the AMS data found between Sierra de las Tunas (base) localities and Sierra de Pillahuincó (top) localities and the differences found in the paleomagnetic studies are coincident. The presence of two different types of syntectonic magnetization at the base and at the top of the sequence of the Tunas Formation indicates a magnetization acquired in different stages, during the folding of the sequence (Tomezzoli, 1997, 1999, 2001; Tomezzoli and Vilas, 1999). In Sierra de Las Tunas area (northwest, Figure 1b), at the base and older sequence with the main deformation, the magnetizations are syntectonic, with unfolding values of 32% (Tomezzoli and Vilas, 1999). In the Sierra de Pillahuincó area (southeast, Figure 1b), at the top and younger sequence, the magnetizations were acquired during the final stages of the

deformation, at the 90 % of the unfolding sequence (Tomezzoli, 2001). On this basis, two different paleomagnetic poles (PPs) were calculated: Tunas I and Tunas II PPs, respectively (Tomezzoli and Vilas, 1999; Tomezzoli, 2001). The Tunas I PP (Tomezzoli and Vilas, 1999) is located at the Early Permian of the apparent polar wander path (APWP) of South America (Tomezzoli, 2009; Gallo *et al.*, 2017) while the Tunas II PP (Tomezzoli, 2001) is placed at the APWP in the Early-Late Permian (Tomezzoli, 2009; Gallo *et al.*, 2017). Paleomagnetic and ASM studies, illite re-crystallization ages (Buggisch, 1987), outcropping different folding geometry in the shortening values, as well as the presence of growth strata (López Gamundi *et al.*, 1995) and deformation structures (Falco and Arzadún, 2012) indicate that during the Permian the region was unsteady. The presence of syntectonic magnetizations with different percentages of unfolding demonstrates that the tectonic shortening diminishes toward the top (Figure 2a). Thus, this sedimentation and folding pattern could propagated toward the east to the foreland basin from the Early to Late Permian (Figure 2b).

Fryklund *et al.* (1996), based on seismic and drilling data, mentioned the existence of Paleozoic sediments on subsurface of the Colorado Basin, to the south of the Buenos Aires province, suggesting the extension of the Claromecó Basin at the south (Figure 1). The records are similar to those that outcrop in the Sierras Australes. Lesta and Sylwan (2005) recognized four depositional cycles in subsurface and they correlated them with “Ventania” and “Tandilia” through drilling and seismic data. Pángaro and Ramos (2012), based on the interpretation of seismic data and gravimetry, calculate a thickness of more than 14 km of Paleozoic sediments for the Claromecó Basin. It would be comparable to the outcropping sedimentary column of the Sierras Australes area.

Sampled localities description

Ruta 76

This sampled locality is on the 76 Provincial Road, at 2 km at the south of El Perdido stream, in the Sierra de las Tunas (37° 53`15`` S, 61° 51`38 W) (Figure 1b). Tomezzoli and Cristallini (1998) interpreted it as a system of drag folds (Figure 3a). This section was also studied with paleomagnetism (Tomezzoli, 1997) and anisotropy of magnetic susceptibility (Arzadún *et al.*, 2016).

At the northwestern section of the outcrop, there is a sequence of 20 m with tabular strata of fine to very fine-grain sandstones of green color that have sharp bases and parallel lamination, showing concretions and hematite nodules. They are interbedded with medium-grain cross bedding sandstones of yellow color, with negative geometries and erosive bases (Figures 3b and 3c). In the middle part of the outcrop, there are layers of red massive mudrocks, with tabular geometries and net bases. In the southern sector, there are 1 m thick strata of fine whitish and orange tuff material, with tabular geometries, net bases, and parallel lamination to massive structure, normal gradation, and loading deformation at the tope (Figure 3d). The strata are northwest-southeast strike with high dip angles. There are veins in the sandstones, perpendicular or parallel to the bedding planes and arranged in the fault planes, filled by quartz.

Similar levels of pyroclastic material had been mentioned and described by Iñiguez *et al.* (1988) in other localities of the Tunas Formation, such as Abra del Despeñadero, Las Julianas and Las Mostazas (Figure 1b).

PANG0001 well

The PANG0001 well is located at 50 km at the north of the Coronel Pringles locality (37º 34 '48' 'S, 61º6'57.35' 'W), into the Claromecó Basin geological area (Figures 1a and 1b). The well cores were donated to the Universidad Nacional del Sur by the Rio Tinto Mining Exploring company for academic purposes. The well reaches 959 m depth under wellhead

(mbw) with a plugs extension of 776 m. In its sequence, the base of the Tunas Formation is not identified, whereas at 191 mbw is the top, although it is covered by discordance with modern material. This indicates a thickness of the Tunas Formation greater than 768 m in the center of the basin (Figure 4).

In the lower section (at the base) of the PANG0001 well, the Tunas Formation is composed of fine-grain sandstones and mudrocks with cross-lamination with net bases, interbedded with black mudrocks containing pyrite nodules (Figures 5a and 5b). In this section one-meter thick coal beds are interbedded (Figures 4 and 5c) (Arzadún *et al.*, 2017). In addition, there are thin boundstones levels of (up to 5 cm thick) belonging to microbial algae (Arzadún *et al.*, 2013, Figure 5d). The mudrocks have sections with important bioturbation and prints of Glossopteris, Gangamopteris, Lycopsids and some charred woody remains (Figures 4, 5a and 5b). Towards the upper section (to the top), there are medium-grain sandstones with erosive bases interbedded with lesser quantity of carbonaceous black and green mudrocks with hematite nodules (Figures 6a and 6b). There are some coal and carbonaceous mudrocks levels, up to 50 cm thick, interbedded in this section (Figure 4). At the base of the well, at 780 mbw, there are up to 6 m thickness of greenish-gray tuffs, with cross and parallel lamination, normal gradation and loading deformation in the roof of some strata (Figures 6c and 6d). In the upper part, at 255 mbw, there are thinner, not exceeding 1 m thick, strata of tuffs (Figure 4). The tuff of the base of the well were dated in this contribution.

Methodology

About 2 kg of pyroclastic material outcropping in the Sierra de Las Tunas were sampled in the Ruta 76 locality, and 2 kg from subsurface, in the PANG0001 well (Figure 1). The samples were petrographically analyzed by optical microscope using a Nikon eclipse 50i POL and by X-ray difraction with a Rigaku Denki Geigerflex Max III C equipment with graphite

monochromator, Cu Kα radiation and 2° per minute sweep velocity. The used equipment is available at the Geology Department, at the Universidad Nacional del Sur.

For SHRIMP analysis, it is necessary at first, to achieve the separation of the zircons. For this purpose, the samples were initially pulverize and sieved with # 35 mesh. Subsequently, with a handheld magnet, the ferromagnetic minerals were extracted and the sample was process with the Frantz magnetic separator at 0.5 and 1.0 Amper. From the non-magnetic fraction, 100 zircons were separated in a Petri dish with alcohol, using the binocular glass and photograph were taken.

The isotopic analysis were carried out in GeoLab-IGc-USP (Centro de Pesquisas Geocronológicas of the Universidad de San Pablo in Brazil), with a SHRIMP IIe equipment. The primary beam analytical conditions are Kohler aperture = 120 μm, spot size = 30 μm, and O^{-2} beam density = around 2.5 – 7 ηA (dependent of brightness aperture). The secondary beam analytical conditions are source slit = 80 μm, mass resolutions for $^{196}(Zr_2O)$, ^{206}Pb, ^{207}Pb, ^{208}Pb, ^{238}U, $^{248}(ThO)$ and ^{254} (UO) ranging between 5,000 and 5,500 (1%), and residues < 0.020 energy slit = open.

About the acquisition table setup, the raster time is 2 – 3 minutes with spot size = 50 μm, plus 0.5 minutes of burning time fixed at the center. Acquisition parameters are: Zr_2O = 2s; ^{204}Pb = 10s; 204.1 = 10s; ^{206}Pb = 10s, ^{207}Pb = 20-30s, ^{208}Pb = 10s, ^{238}U = 10s, $^{248}(ThO)$ = 5s and $^{254}(UO)$ = 5s. About the setup conditions of the acquisition table, primary beam autotune is systematically carried out in the Source Steering Y and Source Steering Z focus lens and secondary beam autotune QT1Y and QT1Z are enabled. Auto run selector is $^{254}(UO)$, in which auto center method is measured at 50% of the peak height. The analytical cycle number is equal to 5 cycles for Neoproterozoic-Archean samples, and equal to 6 – 7 cycles for Phanerozoic samples. All raw count rates have been corrected for a dead time of 25 ns and analytical rate among standard and sample is 1 standard to 4 zircon samples.

The acquisition and data processing was made with U-Pb calibration: the Pb^+ ionization efficiency is about a factor of two higher than U^+, and so the $^{206}Pb^+/^{238}U^+$ ratio must be calibrated by a standard material (Ln (Pb/U) x Ln (UO/U - slope ~2, Williams, 1998). Measured $^{206}Pb^+/^{238}U^+$ varies with the measured UO^+/U^+ to define a calibration line of known age, in this case 416,78 Ma for Temora 2 or 572 Ma for SL13. The age of an unknown sample can then be determined by the ratio of $^{206}Pb^+/U^+$ in the unknown to that ratio in the standard at the common UO/U value. For additional information, see Williams (1998).

SHRIMP softwares are LabVIEW 8.5 and SHRIMP SW, version 2.90. Data was reduced using SQUID 2.5 and ISOPLOT 4 (Ludwig, 2009). Common lead corrections usually use ^{204}Pb according to Stacey and Kramer (1975). Temora 2 is used as $^{206}Pb/^{238}U$ age reference (416.78 Ma, Black *et al.*, 2004), and Z6266 (903 ppm, Stern and Amelin, 2003) is used as U composition reference. Analytical uncertainties are in 1-σ error for each analysis.

Tuffs petrography

Ruta 76

The Ruta 76 samples are composed of rounded grains of quartz, feldspars and lithic fragments corresponding mainly to volcanic rocks and less mudrocks and polycrystalline quartz, with 100 μm average sizes and 200 μm maximum. They contain micas (muscovite and less biotite, the last one chloritized) and epidote, both minerals with similar size to the grains. The matrix, which reaches up to 75% of the rock in a matrix-supported texture, is composed of sericite, silica and minor quantity elongated devitrified glass shards (ash fragments). The cement is composed of brown color iron oxides (Figure 7). The samples have moderate selection and classify as fine tuffs according to Fisher (1961).

PANG0001 well

PANG0001 well samples are composed of rounded grains of quartz and, in minor quantity, feldspar and plagioclase, with average 80 μm sizes. It contains micas (biotite and chloritized muscovite) oriented and bended and elongated pale yellow and brown glass shreds, devitrified and replaced by clays. The matrix, which reaches more than 75% of the sample in a matrix-supported texture, is composed of sericite and silica. There is locally replacement with carbonate cement (Figure 8). The samples have well to moderate selection. They classify as fine tuffs according to Fisher (1961).

The X-ray analysis in both samples show peaks that belonging to quartz, muscovite and smectite (Figure 9) as a product of glass alteration (Tucker, 1981).

Zircon separation

The zircons, separated under binocular glass according to their shape and size, were classified into different groups (Table 1). There are three populations of zircons from the Ruta 76 sample with a total number of 317 zircons. The zircons of population R1 have euhedral shape, R2 have rounded shape and R3 are euhedral shape and smaller size (Figures 10a and 10b). The sample from PANG0001 well have 245 zircons of small size, classified in three populations: P1 are zircons euhedral and elongated, P2 are rounded and P3 are subhedral and have less brightness (Figures 10c and 10d).

U-Pb ages

The obtained ages indicate that Ruta 76 and PANG0001 well samples, situates both at the base of the Tunas Formation, are almost contemporaneous, with 291.7 ± 2.9 and 295.5 ± 8.0

Ma ages, respectively, belonging to the Sakmarian, Lower Permian, according to the time scale of Ogg *et al.* (2016) (Figure 11). These mean ages are controlled by the youngest grains that are predominant in both samples and have mainly euhedral shapes. Nevertheless, in less quantity, there are zircons with rounded shapes that have older ages (Table 2). The Ruta 76 sample has zircons from 1200 to 1800 Ma (Mesoproterozoic) and the PANG0001 well sample contains zircons of 1200 Ma (Figure 11 and Table 2). These zircons could come from other sources as they have rounded shapes and the samples have clastic components. The edges and cores of the grains were separately dated and similar ages were obtained in both, so it can be deduced that these zircons come from parental sources. The Ruta 76 sample presents lower standard deviation than the PANG0001 well sample, because of the minor dispersion of the data (Figure 11 and Table 2).

Results analysis

Due to the alteration degree of the pyroclastic material, especially in rocks of fine grain sizes, it is difficult to analyze their original composition and determine their provenance. In the analyzed samples, there are significant percentage of lithic grains, corresponding to volcanic rocks considered as epiclastic fragments. On the other hand, vitreous fragments are considered as pyroclastic fragments, generated by explosive eruptions.

In the outcrop samples, the percentage of epiclastic fragments is higher than in the PANG0001 well samples. The fine granulometry of the samples and their vitreous composition indicate that an acidic volcanic event ejected this material and it was transported and deposited away from the source area (Walcker and James, 1992). The presence of certain sedimentary structures in these fine tuffs, such as normal gradation, parallel and cross

lamination and deformation by load, as well as the presence of net bases, are indicating that they were deposited in a low energy subaqueous environment.

The tuffs founded in the Claromecó Basin correspond to altered volcanic ash layers with a certain sedimentary rework, as they have rounded grains, lithic fragments and present some poor sedimentary structures. The tuffs are extended for long distances from the Sierras Australes to the Claromecó Basin, where they are interbedded with coal layers (Arzadún *et al*., 2017).

The obtained ages indicate that the Tunas Formation have been deposited between the Sakmarian and Kunguriano (lower Permian), or earlier. The ages of the outcrop tuffs at the base of this formation are similar to the tuffs in subsurface in the Claromecó Basin: 291.7 ± 2.9 Ma and 295.5 ± 8.0 Ma respectively (Figure 11). The mayor standard deviation in the well tuff is because they have more dispersion data (Table 2), maybe due the mayor distance from the source as it is situated at the center of the basin. Zircons with older ages (Mesoproterozoic) are considered inherited from other sources. This study allow to assign the same age to the interbedded coals in the subsurface sequence.

The fact that the obtained ages from the outcrops (Ruta 76 with 291 Ma; Figure 1) are similar to those of the subsurface (PANG0001 well with 295 Ma) implies that the deposition occurs almost contemporaneously in both sectors or that the sedimentation rate during the Lower Permian was high (Andreis *et al.*, 1979). This is common in passive margins and in retro-arc basins (Doglioni *et al.*, 1998), that could be the case of the Claromecó Basin, since it is considered as a foreland basin from the Late Devonian to the Permian (Tomezzoli, 2012).

The ages obtained are agree with the fossil findings of Glossopteris (Archangelsky and Cúneo, 1984), with the palynological contain reported by Balarino (2014), and with the reverse polarity isolated from the base to the top of the Tunas Formation (Tomezzoli and

Vilas, 1999; Tomezzoli, 2001), assigned to the Kiaman superchron (Irving and Parry, 1963), ranging from 318 Ma (Opdyke *et al.*, 2014) to 269 Ma (Lanci *et al.*, 2013).

In the Sierra de Pillahuincó, in the Abra del Despeñadero locality, where is the upper outcrop section of the Tunas Formation (Figure 1b), López Gamundi *et al.* (2013) obtained ages of 280.8 ± 1.9 Ma. In this locality, detrital zircon ages from two samples, record youngest and most important peaks of 291 and 281 Ma respectively (Kunguriano; Ramos *et al.*, 2013; Sato *et al.*, 2015).

Since a regional point of view, tuff levels similar to those of the Tunas Formation were recognized in several basins along the southwestern margin of Gondwana (Figures 12 and 13a). Guerra-Sommer *et al.* (2005, 2008) obtained U/Pb ages of 296.9 and 296.1 Ma in zircons of *tonsteins* interbedded with the Candiota coals, located in the Paraná Basin in Brazil. They correlated them with the Paganzo Basin sequences (with ages of 302 and 288 Ma), the top of the Dwyka tillite (302 and 299 Ma; Matos *et al.*, 2001) and the lower section of the Ecca Group (288 and 289 Ma) in the Karoo Basin. Cagliari *et al.* (2014) obtain U/Pb ages of 290.6 and 281.7 Ma in zircons of *tonsteins* from the Rio Bonito Formation in the Paraná Basin, corresponding to the Sakmariano and Kunguriano and also temporally correlate them with the Dwyka Group, Karoo Basin in South Africa and with the Patquía Formation, Paganzo Basin (Gulbranson *et al.*, 2010), in the northwest of Argentina. Tickyj *et al.* (2010) obtained U/Pb ages of 276 ± 11 Ma in lava flow related to the predecessors of the Choiyoi Group, in La Pampa province, Argentina.

The ages obtained by Cagliari *et al.* (2014), Guerra Sommer *et al.* (2008), Tickyj *et al.* (2010) and the ages obtained in this work are similar, and would be suggesting that the same volcanic event was the source of the volcanic ash fall. In addition, the most modern radiometric ages are similar to those published by Mori *et al.* (2012). According to Lopez-Gamundi (2006), Santos *et al.* (2006), Guerra-Sommer *et al.* (2008), Mori *et al.* (2012) and Sato *et al.* (2015),

the ash fall layers in the Paraná Basin are part of the same episodes located along the Gondwana margin. The U/Pb ages obtained in western Argentina (Figure 1a), indicate that the volcanic activity extended by approximately 30 Ma, from 298 to 251 Ma (Rocha-Campos *et al.*, 2011) and 286 to 247 Ma (Sato *et al.* 2015). Before this period, during the Carboniferous, the magmatic arc was active in the west and along the Paleo-Pacific margin (López-Gamundi *et al.*, 1995; Kleiman and Japas, 2009; Tomezzoli, 2012). The Permian event is associated with the San Rafael orogenic phase (Azcuy and Caminos, 1987), which according to Tomezzoli (2012 and references cited there) it is the result of the final coupling of several continental microplates assembled to the Gondwana that would have previously collided, possibly during the Late Devonian in the Cháñica orogenic phase (Turner and Méndez, 1975). According to the anisotropy of magnetic susceptibility (AMS) studies, there is a variation of the magnetic signature from the SW to the NE, i.e. from the base to the top (Arzadún *et al.*, 2016). The K_{min} axes of AMS, which are arranged along a NE-SO semicircle, move from horizontal positions at the most western sites, at the base of the sequence, indicating a tectonic fabric, to vertical positions at the eastern sites, at the top of the sequence, indicating a fabric with more sedimentary features (Arzadún *et al.*, 2016). This imply a deformation, generated by efforts that come from the southwest decreasing toward the northeast; thus indicates a tectonically active environment during the Permian, where the tuff layers were deposited in some sectors associated with the deposition of coal beds.

The paleomagnetic study, carried out in the Tunas Formation, yield that these rocks carry a very stable characteristic magnetization with a very good internal consistency inside each sampling site. Although the type of magnetization is different at Sierra de las Tunas (base of the sequence) or in the Sierra de Pillahuincó (top of the sequence) (Figure 13b, Tomezzoli and Vilas, 1999; Tomezzoli, 2001). From the average of the final paleomagnetic mean directions per site, with structural corrections, a paleomagnetic pole (PP) of each locality were

calculated. They were grouped into the Tunas I PP that represents the magnetizations for the base (Tomezzoli and Vilas, 1999) and Tunas II PP, which represents the magnetizations for the top of the sequence (Tomezzoli, 2001) (Figure 13b). Both PPs are consistent with the polar wander path of South America proposed by Tomezzoli (2009) and Gallo *et al.* (2017), occupying different positions (Figure 13b), and they are concordant with the structural field differences. Thus, the Tunas I PP (Tomezzoli and Vilas, 1999) remains dated in 291.7 ± 2.9 (in this work) and integrating these results with those of Lopez Gamundi *et al.* (2013) and Alessandretti *et al.* (2013), it is possible assign to Tunas II PP (Tomezzoli, 2001) an age of 280.8 ± 1.9. The differences in the ages of the Tunas I and Tunas II PPs are consistent with all the mentioned geological evidence (sedimentary, petrologic and structural). These data allowed to calculate a northward latitudinal speed of 2.7 cm/year for Gondwana during the Permian (Figure 13a).

Discussion

In this work is reported the finding of pyroclastic material in the base of the Tunas Formation, classified as fine tuffs with some lithic contain, at the outcropping base of the sequence and at the subsurface into the Claromecó Basin. The last ones are interbedded in a sequence that includes coal beds. The radimetric ages obtained from SHRIMP analysis are 291.7 ± 2.9 and 295.5 ± 8.0 Ma respectively, corresponding to the Early Permian (Sakmarian to Kunguriano, according to Ogg *et al.*, 2016, Gradstein *et al.*, 2004). This age can be considered the older possible age of deposition of the sedimentary sequence and the coals that are interbedded in it. This would be indicating a synchronous pyroclastic event with the deposition of the Tunas Formation in all its extension, associated to an acid-type volcanism, probably due to a surtseyan or freatoplinian type eruption (Walcker and James, 1992), in a sub-aqueous low-

energy environment. As the Tunas Formation represent the culmination of the regressive cycle after the carboniferous glaciation, it is also possible to constraint the age of the upper Paleozoic glaciation (represented by the lower part of the Pillahuincó Group).

In the Sierra de Pillahuinco, in the Abra del Despeñadero locality, where outcrop the top of the Tunas Formation, López Gamundi *et al.* (2013) obtained ages of 280.8 ± 1.9 Ma (Arstinkiano, according to Gradstein *et al.*, 2004). In addition, other authors described and dated similar and contemporaneous pyroclastic events in different basins that belong to the southwestern margin of Gondwana, which indicates a regional character of the same one.

The radimetric data was integrate with other geological characteristics, such as syntectonic sedimentation (Lopez Gamundi *et al.*, 2006), two distinct paleomagnetic syntectonic poles (Tomezzoli and Vilas, 1999; Tomezzoli, 2001), differences in the structural and AMS patterns (Arzadún *et al.*, 2017) and deformation structures related with seismic activity (Falco and Arzadún, 2012). All these data indicate a tectonically active and changing environment during the Permian of Gondwana displayed on the Tunas Formation environment. This deformation event is known in Argentina as the San Rafael orogenic phase (Azcuy and Caminos, 1987). On a regional scale, López Gamundi *et al.* (1995) interpreted this deformation and the coeval foreland basin phase as diachronously affecting the entire Panthalassan margin, ranging from the Early Permian in western Argentina, to slightly later in South Africa, to Late Permian in eastern Australia (Veevers *et al.*, 1994).

As pigmented, either detrital grains or both could carry the magnetization in the Tunas Formation and these rocks have not a significant metamorphism (Cobbold *et al.*, 1986; Buggisch, 1987), the magnetization is mainly syn-depositional to syn-diagenetic. Thus, this magnetization and folding pattern indicates that the rocks were remagnetized during a relative short period of time (Figure 2b), as folding more slowly propagated towards the eastern foreland (Figure 2a). Thus, the Tunas I PP (Tomezzoli and Vilas, 1999) remains dated in

291.7 ± 2.9 (this work) and PP Tunas II (Tomezzoli, 2001) in 280.8 ± 1.9 (Lopez Gamundi *et al.*, 2013; Alessandretti *et al.*, 2013). The differences in the ages of the Tunas I and Tunas II PPs are consistent with all the mentioned geological evidence (sedimentary, petrologic and structural). These data allowed to calculate a northward latitudinal speed of 2.7 cm/year for Gondwana during the Permian (Figure 13a). This Permian latitudinal movement would be the consequence of the final coupling of several continental microplates, gradually amalgamated from the southerns margins to Gondwana and from the northern to Laurentia to configure the Pangea. The Pangea continent started its amalgamation as a B-type during the Early Carboniferous and Early Permian to reach its final A-type configurations in the Late Permian (Figure 13b; Gallo *et al.*, 2017).

Since the main accretions in the southwestern margin of Gondwana could have started in the Devonian - Carboniferous, this Permian orogeny (San Rafael Orogenic Phase) would be representing the post-collisional deformation, with a peak of compression in the Early Permian that is would have attenuated towards the foreland during the Late Permian - Early Triassic.

Acknowledgments

We thank to Centro de Pesquisas Geocronológicas of the Universidad de San Pablo (Brazil), for providing the dating necessary equipment and the Geology Department of Universidad Nacional del Sur for providing the necessary equipment for carry out the petrography. Thanks to the Rio Tinto Mining Exploring company for donate the cores of the PANG0001 well. This work was funding through the “Ing. E. Mosconi", "Jorge A. Sábato" technologic-link projects. We thank to Hugo Tickyj, from the La Pampa University, to provide information about the mineral separation and the critic lecture of the manuscript.

Figures

Figure 1. A. Location of the Sierras Australes thrust and fold belt (orange and green) in the southwest of Buenos Aires province, Argentina, developed in the southwestern margin of the Gondwanides belt (in violet) and other surrounding geological provinces (Carapacha Basin, in pink, and Choiyoi magmatic province, in light blue). The studied samples are on the Ruta 76 locality and on the PANG0001 well in the Claromecó Basin, in yellow (Kostadinoff and Font de Affolter, 1982; Fryklund *et al.*, 1996, Alvarez 2004, Zilli *et al.*, 2005, Pángaro and Ramos, 2012). **B.** Geological map of the Sierras Australes, southwest of the Buenos Aires province, Argentina, modified from Suero (1972). The Tunas Formation (orange) outcrops in the Sierra de las Tunas (north) and in the Sierra de Pillahuincó (south). Location of the most important outcrops of the described tuffs: Ruta 76 and Abra del Despeñadero. The paleomagnetic pole Tunas I correspond to the Sierra de las Tunas and Tunas II to the Sierra de Pillahuincó.

Figure 2. A. Diagram showing the shortening percentage for the Tunas Formation. The highest values are at the west, in the base of the sequence (Sierra de las Tunas, Figure 1b), and the smaller values are at the younger and eastern position, in the top of the sequence (Sierra de Pillahuinco Figure 1b). **B.** Relationships between stratigraphic levels, magnetization and deformation of Tunas Formation: whereas the base strata shows simultaneous processes, data at the top strata indicate tectonic magnetization (Tomezzoli, 1999).

Figure 3: **A:** Schematic structural profile of the Tunas Formation outcrops, on the Ruta 76 (see more details in Tomezzoli and Cristallini, 1998). **B:** Regional view of the outcrop. The

red square is the sample position. **C:** Detail of the lithology with yellow sandstones (ss) intercalate with red and green mudrocks (mr). **D:** detail of a polished tuff sample.

Figure 4. Simplified sedimentological profile of the PANG0001 well, showing the lithology, structures, fossils and facies. To the left, photograph of the different lithology. In red, tuff sampled level.

Figure 5. Detailed lithology and structures at the lower section of the PANG0001 well. **A:** Mudrock with sedimentary structure obliterated by bioturbation. **B:** Black mudrock with pyrite nodule filling a fossil track. **C:** Coal sample. **D:** Microbial algae, composing by lamina of carbonate and dark mudrock.

Figure 6. Lithology of the PANG0001 well. **A:** Medium-grain sandstone with erosive base. **B:** Green mudrock with hematite nodules. **C** and **D:** Greenish-gray tuff material with parallel lamination.

Figure 7. Microphotographs of fine tuffs outcropping on the Ruta 76 locality. **A** and **B**: With parallel nicols. **C** and **D**: With crossed nicols. Matrix-supported texture with heterogeneous grain sizes and composition, with shards of glass in the matrix. Qz: quartz. Fv: lithic fragments of volcanic rocks. Ms: muscovite. Tr: shards of glass. Ff: lithic fragments of mudrocks. Bi: biotite. The matrix is composed mostly of silica and sericite. The cement is composed of iron oxides (Fe).

Figure 8. Microphotographs of fine tuffs of the PANG0001 well. **A** and **B:** they are composed of micas, quartz, shards of glass and biotite that is oriented and flexed. **C:**

Carbonate is observed as a replacement for the original minerals. **D:** Matrix-supported texture and non-homogeneous size grain. Qz: quartz. Ms: muscovite. Tr: shards of glass. Bi: Biotite. Ca: carbonate.

Figure 9. X-ray analysis of tuffs corresponding to the Tunas. Ms: muscovite, Sm: smectite, Qz: quartz. All localities present a similar mineralogical composition.

Figure 11. Ages of the samples based on the ^{206}Pb / ^{238}U and ^{207}Pb / ^{238}U ratio with their error ellipsoids in 2σ for each measurement (in orange). **A:** 76 Road sample. **B:** PANG0001 well sample.

Figure 12. Simplified stratigraphic chart showing the Permian formations in different basins that belong to the southwestern margin of Gondwana. The levels of tuffs and tectonic and volcanic episodes are detailed (López Gamundí 2006).

Figure 13. **A.** Paleogeographic reconstructions of Gondwana during the Early Permian along the South West Gondwana margin (modified from Gallo *et al.* 2017). Botton, plate accretion during Permian times. **B.** Apparent polar wander path of the South West Gondwana proposed by Tomezzoli (2009) constructed from the paleomagnetic poles (PPs) selected from South America between the Carboniferous and Triassic, with the ages of both PPs Tunas I and Tunas II.

Tables

Table 1. Description and quantity of zircons from different groups in the samples belonging to the Ruta 76 locality and the PANG0001 well.

Table 2. Sumary of SHRIMP U-Pb zircons of the two samples of the Tunas Formation. In orange, the older zircons that are considered as detritic.

References

Alessandretti, L., Philipp, R.P., Chemale, F., Brückmann, M.P., Zvirtes, G., Metté, V. and Ramos, V.A., 2013. Provenance, volcanic record, and tectonic setting of the Paleozoic Ventania Fold Belt and the Claromecó Foreland Basin: implications on sedimentation and volcanism along the southwestern Gondwana margin. Journal of South American Earth Sciences. 71 pp.

Álvarez, G.T., 2004. Cuencas Paleozoicas asociadas a la prolongación norte del sistema de Sierras de Ventania, Provincia de Buenos Aires. PhD thesis. Universidad Nacional del Sur. Argentina.

Amos, A.J., 1980. Correlación de las formaciones carbonáticas y pérmicas marinas de Argentina. Brazilian Sciences Academy, Annals. 53(2): 347-356.

Amos, A.J. and Urien, C.M., 1968. La falla "Abra de la Ventana" en las Sierras Australes de la provincia de Buenos Aires. Revista de la Asociación Geológica Argentina, 23(3): 197-206.

Andreis, R.R., 1984. Análisis litofacial de la Formación Sauce Grande (Carbónico superior?), Sierras Australes, provincia de Buenos Aires. Anual Meeting Project 211-IGCP, "Late Paleozoic of South America", San Carlos de Bariloche, Río Negro, Argentina. pp. 28-29.

Andreis, R.R., Lluch, J.J. and Iñiguez Rodríguez, A.M., 1979. Paleocorrientes y paleoambientes de las Formaciones Bonete y Tunas, Sierras Australes de la Provincia de Buenos Aires, Argentina. Actas 6° Congreso Geológico Argentino. 2: 207-224.

Andreis, R.R., Iñiguez Rodríguez, A.M., Lluch, J.J. and Rodríguez, S., 1989. Cuenca paleozoica de ventania. Sierras Australes de la provincia de Buenos Aires. En: Chebli, G. Spalletti, L. (Eds.): Cuencas sedimentarias argentinas. Serie Correlación Geológica. 6:265-298.

Andreis, R.R. and Cladera, G., 1992. Las epiclastitas pérmicas de la Cuenca Sauce Grande (Sierras Australes, Buenos Aires, Argentina). Parte 1: Composición y procedencia de los detritos. Actas 4º Reunión de Sedimentología. 1: 127-134.

Andreis, R.R. and Japas, S., 1996. Cuencas Sauce Grande y Colorado. In: S. Archangelsy (Ed.), El Sistema Pérmico en la República Argentina y en la República Oriental del Uruguay. Academia Nacional de Ciencias. 45-64.

Archangelsky, S., Azcuy, C.L., González, C.R. and Sabattini, N., 1987. Correlación general de biozonas. En: S. Archangelsky (Ed.), El Sistema Carbonífero en la República Argentina. Academia Nacional de Ciencias. 281-292. .

Archangelsky, S. and Cúneo, R., 1984. Zonación del Pérmico continental de Argentina sobre la base de sus plantas fósiles, 3º Congreso latinoamericano Paleontológico, México. pp. 143-153.

Arzadún, G., Cisternas, M.E., Cesaretti, N.N. and Tomezzoli, R.N., 2017. Presence of charcoal as evidence of paleofires in the Claromecó Basin, Permian of Gondwana, Argentina: Diagenetic and paleoenvironment analysis based on coal petrography studies. GeoRes Journal. 14: 121-134.

Arzadún, G., Tomezzoli, R.N. and Cesaretti, N.N., 2016. Tectonic insight based on anisotropy of magnetic susceptibility and compaction studies in the Sierras Australes thrust and fold belt (southwest Gondwana boundary, Argentina). Tectonics. 35(4): 1015-1031.

Arzadún, G., Tomezzoli, R.N. and Cesaretti, N.N., 2013. Análisis de anisotropía de susceptibilidad magnética (AMS) y compactación en la Formación Tunas, Sierras Australes de la Provincia de Buenos Aires, Argentina. Latinmag Letters Proceedings, Volume 3, Special Issue. 1-6.

Azcuy, C.L. and Caminos, R. 1987. Diastrofismo. In Archangelsky, S., (ed.) El Sistema Carbonífero en la República Argentina, Academia Nacional de Ciencias. 239-251.

Balarino, L., 2014. Permian palynostratigraphy of the Claromecó Basin, Argentina. Alcheringa, 38.

Black, L. P., Kamo, S. L., Allen, C. M., Davis, D. W.,Alenikoff, J. N., Valley, J. W., Mundif, R., Campbell, I. H., Korsch, R. J., Williams, I. S. and Foudoulis C., 2004. Improved 206Pb238U microprobe geochronology by the monitoring of trace element related matrix effect; SHRIMP, ID-TIMS, ELA-ICP-MS and oxygen isotope documentation for a series of zircon standards. Chemical Geology. 205(1): 115-140.

Buggisch, W. E., 1987. Stratigraphy and Very Low Grade Metamorphism of the Sierras Australes de la Provincia de Buenos Aires (Argentina) and Implications in Gondwana Correlation. Zbl. Geol. Paläont. Teil I (7/8): 819-837.

Cagliari, J., Correa Lavina, E.L., Philipp, R.P., Wohnrath Tognoli, F.M., Stipp Basei, M.A. and Faccini, U.F., 2014. New Sakmarian ages for the Rio Bonito formation (Paraná Basin, southern Brazil) based on LA-ICP-MS U/Pb radiometric dating of zircons crystals. Journal of South American Earth Sciences. 56: 265-277.

Chernicoff, C.J., Zappettini, E.O., Santos J.O.S., McNaughton, N.J. and Belousova E., 2013. Combined U-Pb SHRIMP and Hf isotope study of the Late Paleozoic Yaminué Complex, Rio Negro Province, Argentina: implications for the origin and evolution of the Patagonia composite terrane. Geoscience Frontiers. 4: 37-56.

Coates, D.A., 1969. Stratigraphy and sedimentation of the Sauce Grande Formation, Sierra de la Ventana, Southern Buenos Aires Province, Argentina. En A. J. Amos (Ed.), Gondwana Stratigraphy, Unesco, Paris. 799-816.

Cobbold, P., Gapais, D. and Rossello, E., 1991. Partitioning of transpressive motions within a sigmoidal foldbelt: the Variscan Sierras Australes, Argentina. Journal of Structural Geology. 13: 743-758.

Cobbold, P.R., Massabie, A.C. and Rossello, E.A., 1987. Hercynian wrenching and thrusting in the Sierras Australes Foldbelt, Argentina. Hercynica. 2(2): 135-148.

Cobbold, P.R., Massabie, A.C. and Rossello, E.A., 1986. Hercynian wrenching and thrusting in the Sierras Australes Foldbelt, Argentina. Hercynica. 2(2): 135-148.

Di Pasquo, M., Martínez, M.A. and Freije, H., 2008. Primer registro palinológico de la Formación Sauce Grande (Pennsylvaniano-Cisuraliano) en las Sierras Australes, provincia de Buenos Aires, Argentina. Ameghiniana. 45 (1).

Doglioni, C., D´Agostino, N. and Mariotti, G., 1998. Normal faulting vs regional subsidence and sedimentation rate. Marine and Petroleum Geology. 15: 737-750.

Du Toit, A.L., 1927. A Geological Comparison of South America with South Africa. Carnegie Inst. Publ. N. 381, 157 p.

Falco, J.I. and Arzadún, G., 2012. Estructuras de deformación en la Formación Tunas, en la Cantera Las Mostazas, Sierra de Pillahuincó, Sierras Australes de la Provincia de Buenos Aires. XIII Reunión Argentina de Sedimentología, Salta, Argentina. 73-74.

Fielding, C.R., Frank, T.D., Birgenheier, L.P., Rygel, M.C., Andrew, T.J. and Roberts J., 2008. Stratigraphic imprint of the Late Paleozoic Ice Age in eastern Australia: A record of alternating glacial and nonglacial climate regime. Journal of the Geological Society. 165:1.

Fisher, R.V., 1961. Proposed classification of volcaniclastic sediments and rocks. Geol. Soc. Amer. Bull. 72: 1409-1414.

Frank, T.D., Schultis, A.l., and Fielding, C.R., 2015. Acme and demise of the late Palaeozoic ice age: a view from the southeastern margin of Gondwana. Paleogeography, Palaeoclimatology and Palaeoecology. 418: 176-192.

Fryklund, B., Marshall, A. and Stevens, J., 1996. Cuenca del Colorado. XIII Congreso Geológico Argentino y III Congreso de Exploración de Hidrocarburos. Geología y Recursos Naturales de la Plataforma Continental Argentina. Eds: V.A. Ramos y M.A. Turic. Relatorio. 8: 135-158.

Furque, G., 1973. Descripción geológica de la Hoja 34n, Sierra de Pillahuincó, Provincia de Buenos Aires. Boletín del Servicio Nacional de Minería y Geología, Buenos Aires. 141, 70 pp.

Gallo, L. C., R. N. Tomezzoli, and E. O. Cristallini, 2017. A pure dipole analysis of the Gondwana apparent polar wander path: Paleogeographic implications in the evolution of Pangea, Geochem. Geophys. Geosyst. 18: 1499-1519.

Gradstein, F.M., Ogg, J. G. and Smith, A. G., 2004. A Geologic Time Scale 2004, Cambridge University Press.

Gregori, D.A., Grecco, L.E. and Llambías, E.J., 2003. El intrusivo López Lecube: Evidencias de magmatismo alcalino Gondwánico en el sector sudoeste de la provincia de Buenos Aires, Argentina. Revista de la Asociación Geológica Argentina. 58: 167-175.

Gregori, D.A., Kostadinoff, J., Strazzere, L. and Raniolo, A., 2008. Tectonic significance and consequences of the Gondwanide orogeny in northern Patagonia, Argentina. Gondwana Research, Elsevier. 14: 429-450.

Guerra-Sommer, M., Cazzulo-Klepzig, M., Formoso, M.L., Menegat, R. and Basei, M.A.S., 2005. New radiometric data from ash fall rocks in Candiota coal-bearing strata and the palynostratigraphic framework in southern Parana´ Basin (Brazil). Abstracts Gondwana. 12, 189.

Guerra-Sommer, M., Cazzulo-Klepzig, M., Laquintinie Formoso, M.L., Menegat R. and Mendonça Fo, J.G., 2008. U–Pb dating of tonstein layers from a coal succession of the southern Paraná Basin (Brazil): A new geochronological approach. Gondwana Research. 14: 474-482.

Gulbranson, E.L., Montañez, I.P., Schmitz, M.D., Limarino, C.O., Isbell, J.K., Marenssi, S.A. and Crowley, J.L., 2010. High-precision UePb calibration of Carboniferous glaciation and climate history, Paganzo Group, NW Argentina. Geol. Soc. Am. Bull. 122: 1480-1498.

Harrington, H.J., 1947. Explicación de las Hojas Geológicas 33m y 34m, Sierras de Curamalal y de la Ventana, Provincia de Buenos Aires. Servicio Nacional de Minería y Geología, Bulletin 61.

Harrington, H.J., 1955. The Permian "Eurydesma fauna of Eastern Argentina. Journal of Paleontology. 29(1): 112-128.

Harrington, H.J., 1972. Sierras Australes de Buenos Aires. In: A.F. Leanza (dir y ed.), Geología Regional Argentina. Academia Nacional de Ciencias. p.401.

Harrington, H.J., 1980. Sierras Australes de la Provincia de Buenos Aires. In: Turner, J.C.M., coord., Geología Regional Argentina, Academia Nacional de Ciencias, Córdoba (Reimpresión de Harrington, 1972a). 2: 967-983.

Iñiguez, A.M., Andreis, R.R. and Zalba P.A., 1988. Eventos piroclásticos en la Formación Tunas (Pérmico), Sierras Australes, Provincia de Buenos Aires. Actas II, Jornadas Geológicas Bonaerenses. 383-395.

Irving, E., and Parry, L. G., 1963). The magnetism of Some Permian Rocks from New South Wales, Geophys. J. R. Astron. Soc. 7(4): 395-411.

Isbell, J.L., Miller, M.L., Wolfe, K.L., and Lenaker, P.A., 2003. Timing of late Paleozoic glaciation in Gondwana: Was glaciation responsible for the development of northern hemisphere cyclothems?, in Chan, M.A., and Archer, A.W., eds., Extreme Depositional Environments: Mega End Members in Geologic Time: Geological Society of America Special

Paper. 370: 5-24.

Japas, M.S., 1986. Caracterización geométrico-estructural del Grupo Pillahuincó. I. perfil del arroyo Atravesado. Sierra de Las Tunas, Sierras Australes de Buenos Aires. Academia Nacional de Ciencias Exactas, Físicas y Naturales. Buenos Aires, Anales. 38:145-156.

Japas, M.S., 1995a. Evolución estructural de la porción austral del arco de las Sierras Australes de Buenos Aires. Revista de la Asociación Geológica Argentina. 49(3): 368-372.

Japas, M.S., 1995b. El Arco Noroccidental de las Sierras Australes de Buenos Aires: Producto de mega kinks extensionales durante el proceso de la deformación? Actas 4° Jornadas Geológicas Bonaerenses. 1: 257-263.

Japas, M.S., 1999. Revisión de las teorías acerca del origen del arco de las Sierras Australes de Buenos Aires. Revista de la Asociación Geológica Argentina. 54(1): 9-22.

Keidel, J., 1916. La geología de las Sierras de la provincia de Buenos Aires y sus relaciones con las montañas del Cabo y los Andes. Min. Agric. Nac., An. Dir. Nac. Geol. Min., IX, 3.

Kilmurray, J.O., 1975. Las Sierras Australes de la Provincia de Buenos Aires, las facies de deformación y nueva interpretación estratigráfica, Revista de la Asociación Geológica Argentina. 30(4): 331-348.

Kleiman, L.E., and Japas, M.S., 2009. The Choiyoi volcanic province al 34ºS-36ºS (San Rafael, Mendoza, Argentina): Implications for the Late Paleozoic evolution of the southwestern margin of Gondwana. Tectophysics. 473: 283-299.

Kostadinoff, J., 1993. Geophysical evidence of a Paleozoic Basin in the interhilly area of Buenos Aires Province, Argentina. Comptes Rendus XII ICCP. 1: 397-404.

Kostadinoff, J., 2007. Evidencia geofísica del umbral de Trenque Lauquen en la extensión norte de la Cuenca de Claromecó, Provincia de Buenos Aires. Revista de la Asociación Geológica Argentina. 62(1): 69-75.

Kostadinoff, J. and Font de Affolter, G. 1982. Cuenca Interserrana Bonaerense, Argentina. 5º Congreso Latinoamericano de Geología, Actas. 4: 105-121,

Kostadinoff, J. and Prozzi, C., 1998. Cuenca de Claromecó. Revista de la Asociación geológica Argentina. 53(4): 461-468.

Lanci, L., E. Tohver, Wilson, A. and Flint, S., 2013. Upper Permian magnetic stratigraphy of the lower Beaufort Group, Karoo Basin, Earth Planet. Sci. Lett. 375: 123-134.

Lesta, P. and Sylwan, C., 2005. Cuenca de Claromecó. VI Congreso de Exploración y Desarrollo de Hidrocarburos. Simposio Frontera Exploratoria de la Argentina. Eds: Chebli, G.A., Cortiñas, J.S., Spalletti, L.A., Legarreta, L., Vallejo, E.L. 217-231

Llambías E.J. and Prozzi, C. R. 1975. Ventania. 6º Congreso Geológico Argentino. Relatorio, Buenos Aires. 79-102.

Llambías E.J., Quenardelle, S., and Montenegro, T., 2003. The Choiyoi Group from central Argentina: a subalkaline transitinal to alkaline association in the cratón adjacent to the active margin of the Gondwana continent. 16(4): 243-257.

López Gamundi, O.R., Alvarez, L., Andreis, R.R., Bossi, G.E., Espejo, I.S., Fernández-Seveso, Kokogian, D., Lagarreta, L., Limarino, C.O. and Sessarego, H., 1989. Cuencas intermontanas. In: Cuencas Sedimentarias Argentinas. Eds: Chebli, G.A. and Spalletti, L.A., 6: 123-68.

López Gamundi, O.R., 1996. Modas detríticas del Grupo Pillahuincó (Carbonífero tardío-Pérmico), Sierras Australes de la Provincia de Buenos Aires: su significado geotectónico, Revista de la Asociación Argentina de Sedimentología. 3(1): 1-10.

López Gamundi, 2006. Permian plate margin volcanism and tuffs in adjacent basins of west Gondwana: Age constraints and common characteristics. Journal of South American Earth Sciences 22: 227-238

López Gamundi, O.R., Conaghan, P.J., Rossello, E.A. and Cobbold, P.R., 1995. The Tunas Formation (Permian) in the Sierras Australes Foldbelt, east central Argentina: evidence for syntectonic sedimentation in a foreland basin. Journal of South American Eatrh Sience. 8 (2): 129-142.

López Gamundi, O.R., Fildani, A., Weislogel, A. and Rossello, E., 2013. The age of the Tunas Formation in the Sauce Grande basin-Ventana foldbelt (Argentina): implications for the Permian evolution of the southwestern margin of Gondwana. Journal of South American Earth Sciences. 45: 250-258.

Ludwig, K.R., 2003. User's Manual for Isoplot/Ex v. 3.0, A Geochronological Toolkit for Microsoft Excel. Berkley Geo- chronology Center Special Publication No. 4, Berkeley, CA.

Matos, S.L.F., Yamamoto, J.K., Riccomini, C., Hachiro, J. and Tassinari, C.C.G., 2001. Absolute dating of Permian Ash-Fall in the Rio Bonito Formation, Paraná Basin, Brazil. Gondwana Research. 4: 421-426.

Montañez, I.P. and Poulsen, C.J., 2013. The Late Paleozoic Ice Age: An Evolving Paradigm. Annual Review of Earth and Planetary Sciences. 41: 629-656.

Monteverde, A., 1937. Nuevo yacimiento de material pétreo en González Chaves. Revista Minera. 8: 116-124.

Mori, A.L.O., Souza, P.A., Marques, J.C. and Lopes, R.C., 2012. A new U-Pb zircon age dating and palynological data from a Lower Permian section of the southernmost Paraná Basin, Brazil: biochronostratigraphical and geochronological implications for Gondwanan correlations. Gondwana Research. 21: 654-669.

Ogg, J.G., Ogg, G., and Gradstein, F.M., 2016. A concise geologic time scale. Ed. Elsevier. 240 pp.

Opdyke, N. D., P. S. Giles and Utting, J., 2014. Magnetic polarity stratigraphy and palynostratigraphy of the Mississippian-Pennsylvanian boundary interval in eastern North America and the age of the beginning of the Kiaman, Bull. Geol. Soc. Am. 126 (7-8): 1068-1083.

Pángaro, F. and Ramos, V.A., 2012. Paleozoic crustal blocks of onshore and offshore central Argentina: Newpieces of the southwestern Gondwana collage and their role in the accretion of Patagonia and the evolution of Mesozoic south Atlantic sedimentary basins. Marine and Petroleum Geology. Ed. Elsevier. 1-22.

Pángaro, F., Ramos, V.A. and Pazos, P.J., 2015. The Hesperides basin: a continental-scale upper Palaeozoic to Triassic basin in southern Gondwana. Basin Research. 1-27.

Ramos, V.A., 1984. Patagonia: un nuevo continente paleozoico a la deriva?. 9° Congreso Geológico Argentino, Actas 2. 311-325.

Ramos, V.A., Chemale, F., Naipauer, M. and Pazos, P.J., 2013. A provenance study of the Paleozoic Ventania System (Argentina): Transient complex sources from Western and Eastern Gondwana Research. 26: 719-740.

Rapalini, A.E., 2005. The accretionary history of southern South America from the latest Proterozoic to the Late Paleozoic: some paleomagnetic constraints. In: Vaughan, A.P.M., Leat, P.T., Pankhurst, R.J. (Eds.), Terrane Processes at the Margins of Gondwana. Geological Society, London, Special Publications. 246: 305–328.

Rapalini, A.E., López de uchi, M., Tohver, E. and Cawood, P.A., 2013. The South American ancestry of the North Patagonian Massif: geochronological evidence for an autochthonous origin? Terra Nova. 25 (4): 337-342.

Rocha-Campos, A. C., Basei, M. A., Nutman, A. Phillip., Kleiman, L. E., Varela, R., Llambias, E., Canile, F. M. and da Rosa, O., 2011. 30 million years of Permian volcanism recorded in the Choiyoi igneous province (W Argentina) and their source for younger ash fall deposits in the Parana Basin: SHRIMP U-Pb zircon geochronology evidence. Gondwana Research. 19 (2): 509-523.

Rocha Campos, A.C. and Carvalho, R.G., 1975. Two new bivalves from the Permian "Eurydesma Fauna" of Eastern Argentina: Boletim Instituto Geologico, Universidade Sao Paulo (Sao Paulo, Brazil). 6: 181-191.

Rossello, E.A. and Massabie, A.C., 1981. Micro y meso estructuras en las Formaciones Lolén y Sauce Grande y sus implicancias tectónicas en las Sierras Australes de la Provincia de Buenos Aires. Revista de la Asociación Geológica Argentina. 36(3): 272-285.

Rossello, E.A. and Massabie, A.C., 1992. Caracterización tectónica del kinking mesoscópico de las Sierras Australes de Buenos Aires. Revista de la Asociación Geológica Argentina. 47 (2): 179-187.

Ruiz, L. and Bianco, T., 1985. Presencia de restos de Lycopsidas arborescentes en Las Mostazas, Paleozoico Superior de las Sierras Australes, Provincia de Buenos Aires. Primeras

Jornadas Geológicas Bonaerenses, Tandil. Comisión de Investigaciones Científicas de la Provincia de Buenos Aires. 217 pp.

Santos, R.V., Souza, P.A., Alvarenga, C.J.S., Dantas, E.L., Pimentel, M.M., Oliveira, C.G. and Araújo, L.M., 2006. Shrimp U–Pb zircon dating and palynology of bentonitic layers from the Permian Irati Formation, Paraná Basin, Brazil. Gondwana Research. 9(4): 456-463.

Sato, K., Basei, M.A.S., Ferreira, C.M., Sproesser, W.M., Vlach, S.R.F., Ivanuch, W. and Onoi, A.T. 2011. U-Th-Pb analyses by excimer laser ablation/ICP-MS on MG Brazilian xenotime. Goldschmidt-2011. Mineralogical Magazine. 1801 pp.

Sato, A.M., Llambías, E.J., Basei, A.S. and Castro, C.E., 2015. Three stages in the Late Paleozoic to Triassic magmatism of southwestern Gondwana, and the relationships with the volcanogenic events in coeval basins. Journal of South American Earth Sciences. 63: 48-69.

Stacey, J. S. and Kramers, J. D., 1975. Approximation of terrestrial lead isotope evolution by a two-stage model. Earth and Planetary Science Letters. 26(2): 207-221.

Stern R. A. and Amelin Y., 2003. Assessment of errors in SIMS zircon U-Pb geochronology using natural zircon standard and NIST SRM 610 glass. Chemical Geology. 197 (1): 111-142.

Suero, T., 1972. Compilación geológica de las Sierras Australes de la provincia de Buenos Aires. Ministerio de Obras Públicas, LEMIT, División Geología, Anales. 3: 135-147.

Tickyj, H., Tomezzoli, R., Chemale, F. and Rapalini, A., 2010. Litología y edad de las volcanitas del Cerro El Centinela, provincia de La Pampa. 10º Congreso de Mineralogía y Metalogenia. Resúmenes. Río Cuarto.

Tomezzoli, R.N., 1997. Geología y Paleomagnetismo en el ámbito de las Sierras Australes de la provincia de Buenos Aires. PhD thesis. Universidad de Buenos Aires, 306 p.

Tomezzoli, R.N., 1999. La Formación Tunas en las Sierras Australes de la Provincia de Buenos Aires. Relaciones entre sedimentación y deformación a través de su estudio paleomagnético. Revista de la Asociación Geológica Argentina. 54 (3): 220-228.

Tomezzoli, R.N, 2001. Further Palaeomagnetic results from the Sierras Australes fold and thrust belt, Argentina. Geophysical Journal International. 147: 356-366.

Tomezzoli, R.N., 2009. The Apparent Polar Wander Path for South America during the Permian-Triassic. Gondwana Research. 15: 209-215.

Tomezzoli, R.N., 2012. Chilenia y Patagonia: ¿un mismo continente a la deriva? Revista de la Asociación Geológica Argentina. 69 (2): 222-239.

Tomezzoli, R.N. and Cristallini, E.O., 1998. Nuevas evidencias sobre la importancia del fallamiento en la estructura de las Sierras Australes de la Provincia de Buenos Aires. Revista de la Asociación Geológica Argentina. 53(1): 117-129.

Tomezzoli, R.N. and Cristallini, E.O., 2004. Secciones estructurales de las Sierras Australes de la provincia de Buenos Aires: repetición de la secuencia estratigráfica a partir de fallas inversas? Revista de la Asociación Geológica Argentina. 59: 330-340.

Tomezzoli, R.N. and Vilas, J.F., 1997. Paleomagnetismo y fábrica magnética en aforamientos cercanos a las Sierras Australes de la provincia de Buenos Aires (López Lecube y González Chaves). Revista de la Asociación Geológica Argentina. 52: 419-432.

Tomezzoli, R.N and Vilas, J. F., 1999. Paleomagnetic constraints on age of deformation of the Sierras Australes thrust and fold belt, Argentina. Geophysical Journal International. 138: 857-870.

Tucker, M.E., 1981.Sedimentary petrology: An introduction. Blackwell Scientific Publications.

Turner, J.C. and Méndez, V., 1975. Geología del sector oriental de los departamentos de Santa Victoria e Iruyá, provincia de Salta, Argentina. Academia Nacional de Ciencias de Córdoba, Boletín. 51: 11-24.

Veevers, J.J., Conaghan, P.J. and Powell, C.McA., 1994. Eastern Australia. In: Veevers, J.J. and Powell, C.McA. (editors), Permian-Triassic basins and foldbelts along the Panthalassan margin of Gondwanaland. Geological Society of America, Memoir. 184: 11-171.

Von Gosen, W., Buggisch, W. and Dimieri, L.V., 1990. Structural and metamorphic evolution of the Sierras Australes (Buenos Aires Province/Argentina). Geologisches Rundschau. 79(3): 797-821.

Von Gosen, W., Buggisch, W. and Krumm, S., 1991. Metamorphism and deformation mechanisms in the Sierras Australes fold and thrust belt (Buenos Aires Province, Argentina). Tectonophysics. 185: 335-356.

Walker R.G. and James N.P., 1992. Facies models. Response to sea level change. Geological Association of Canada. 409 pp.

Williams, I.S., 1998. U-Th-Pb geochronology by ion microprobe. In: M. A. McKibben, I. Shanks, W. C. P. Ridley, W. I. Ridley (Eds.), Application of Microanalytical Techniques to Understanding Mineralizing Process. Reviews in Economic Geology. 7: 1-35.

Zambrano, J.J., 1974. Cuencas sedimentarias en el subsuelo de la provincia de Buenos Aires y zonas adyacentes. Revista de la Asociación Geológica Argentina. 29: 443-469.

Zavala, C.A., Santiago, M.F. and Amaolo, G.E., 1993. Depósitos fluviales de la Formación Tunas (Pérmico). Cuenca Paleozoica de Ventania, Provincia de Buenos Aires. Revista de la Asociación Geológica Argentina. 48 (3-4): 307-316.

Zilli, N., Vallejo, E., Pelliza, H. and Dos Santos, P., 2005. El esfuerzo exploratorio en Argentina. En Chebli, G., Cortiñas, J.S., Spalletti, L.A., Legarreta, L y Vallejo, E.L. (editores): Simposio frontera Exploratoria de la Argentina. VI Congreso de Exploración y Desarrollo de Hidrocarburos. 5-40 p.

Zorzano, A., Di Meglio, M., Zavala, C. and Arcuri, M.J., 2011. La Formación Tunas (Pérmico) en la Cuenca Interserrana. Primera correlación entre campo y subsuelo mediante registros de rayos gamma. XVIII Congreso Geológico Argentino, Actas. Neuquén. 2-6.

Locality	Location	Group	Characteristics	Size (μm)	Quantity	Total
Ruta 76	Sierra de las Tunas, Sierras Australes	R1	euhedrals, translucent, high brightness	180	100	317
		R2	rounded, translucent, high brightness	167	102	
		R3	small size, euhedrals in appearance, high brightness	115	115	
PANG0001	Claromecó Basin	P1	small size, elongated, euhedrals in appearance, high brightness	70	21	245
		P2	small size, rounded, high brightness	90	155	
		P3	subhedrals, less brightness	50	69	

Grain, spot	U (ppm)	Th (ppm)	Th/U	$^{232}Th/^{238}U$	% err	$^{206}Pb/^{238}U$	% err	$^{208}Pb/^{232}Th$	% err	$^{206}Pb/^{238}U$ Age	1σ err	$^{206}Pb/^{238}U$ Age	1σ err	$^{206}Pb/^{238}U$ Age	1σ err	$^{207}Pb/^{206}Pb$ Age	1σ err	$^{208}Pb/^{232}Th$ Age	1σ err	$^{208}Pb/^{232}Th$ Age	1σ err	$^{207}Pb/^{206}Pb$ Age	1σ err
Ruta 76																							
1,1	1126	150	0,14	0,14	0,72	0,062	1,8	0,021	2,7	388	7	388	7	390	7	374	41	310	19	318	18	511	27
2,1	1047	471	0,46	0,46	0,15	0,084	1,8	0,031	2,0	500	9	499	9	513	10	562	65	310	16	295	10	1221	22
3,1	472	537	1,17	1,17	0,18	0,048	1,7	0,015	2,0	301	5	301	5	302	6	300	63	294	7	294	6	454	107
4,1	140	140	1,04	1,04	0,32	0,058	1,8	0,039	4,0	275	8	274	5	289	9	282	864	196	40	196	27	1472	329
5,1	783	150	0,20	0,20	0,85	0,067	1,9	0,023	4,8	411	8	411	8	415	8	448	59	295	25	279	21	702	38
6,1	508	157	0,32	0,32	0,63	0,047	1,6	0,016	2,7	292	5	292	5	294	5	314	78	253	15	249	8	536	33
7,1	535	299	0,58	0,58	1,13	0,066	1,6	0,025	2,4	401	6	400	6	404	7	423	109	368	17	364	10	658	46
8,1	408	343	0,87	0,87	2,17	0,047	1,6	0,017	4,8	293	5	293	5	293	6	301	126	294	16	294	14	282	216
9,1	228	145	0,66	0,66	0,96	0,342	2,2	0,118	2,7	1895	36	1910	41	1865	39	1781	12	2256	58	2452	93	1479	32
10,1	281	94	0,35	0,35	1,46	0,055	1,7	0,021	4,3	335	6	335	6	338	6	355	252	292	36	288	36	581	152
11,1	200	76	0,39	0,39	0,37	0,066	2,5	0,028	4,8	403	10	402	10	402	11	457	149	419	32	408	29	375	105
12,1	442	306	0,71	0,71	0,39	0,069	1,8	0,024	4,4	419	7	418	7	426	9	456	157	353	21	348	20	959	93
13,1	151	202	1,39	1,39	0,92	0,049	2,4	0,019	4,0	293	7	293	7	290	10	287	421	302	18	302	16	-39	976
14,1	485	866	1,84	1,84	0,18	0,058	2,7	0,019	2,9	356	10	356	10	363	14	388	156	338	11	337	10	926	303
15,1	225	138	0,63	0,63	0,36	0,050	1,7	0,015	5,0	308	5	308	5	316	6	339	171	229	19	226	13	1052	54
16,1	319	157	0,51	0,51	4,62	0,204	2,1	0,043	9,7	1182	23	1180	24	1219	25	1218	66	646	79	615	69	1781	55
17,1	400	465	1,20	1,20	0,27	0,058	2,0	0,019	4,2	348	7	348	7	363	9	360	342	274	21	274	14	1415	209
18,1	281	136	0,50	0,50	0,34	0,051	1,7	0,018	5,6	316	5	316	5	317	6	339	149	308	22	305	21	408	97
19,1	305	195	0,66	0,66	1,35	0,089	1,9	0,017	3,5	542	10	543	10	573	11	538	105	252	20	253	12	1675	31
20,1	163	150	0,95	0,95	0,32	0,045	1,8	0,011	7,3	276	5	276	5	293	6	269	254	170	17	170	15	1625	123
21,1	167	143	0,88	0,88	0,35	0,047	1,7	0,016	3,0	291	5	291	5	294	6	301	225	270	16	269	9	645	105
22,1	157	67	0,44	0,44	0,52	0,048	1,8	0,017	4,8	297	6	297	6	300	6	310	288	256	29	255	29	620	163
23,1	347	76	0,23	0,23	0,70	0,062	2,0	0,025	3,2	386	8	386	8	387	8	384	138	349	33	350	37	490	96
24,1	508	387	0,79	0,79	1,37	0,053	1,6	0,015	2,9	325	5	325	5	336	6	362	170	241	14	238	9	1212	63
25,1	234	73	0,32	0,32	0,40	0,067	1,7	0,024	7,0	415	7	414	7	414	7	434	69	423	33	418	30	399	50
25.1b	179	165	0,95	0,95	0,34	0,047	2,4	0,018	3,3	284	7	283	7	285	8	317	345	276	19	274	14	462	209
26,1	270	403	1,54	1,54	0,24	0,046	2,6	0,015	3,0	284	7	284	7	287	10	270	214	273	10	274	10	623	344
27,1	221	117	0,55	0,55	0,71	0,237	1,7	0,071	3,3	1363	21	1361	23	1373	23	1391	33	1221	48	1192	47	1540	30
28,1	223	53	0,25	0,25	1,05	0,048	2,3	0,018	5,4	300	7	300	7	302	7	303	164	232	38	231	19	581	58
29,1	185	137	0,77	0,77	1,29	0,046	1,8	0,018	3,2	283	5	283	5	284	6	297	283	273	18	272	15	457	176
30,1	735	281	0,40	0,40	0,27	0,053	2,0	0,016	2,7	320	6	320	6	336	7	262	154	63,3	23	72,2	7	1432	21
31,1	118	127	1,10	1,10	0,48	0,064	3,6	0,017	8,0	366	14	366	13	412	17	412	644	127	41	124	26	2312	136
32,1	377	63	0,17	0,17	0,44	0,063	2,0	0,024	7,9	391	7	390	7	392	8	421	68	349	40	335	31	511	45
33,1	201	120	0,62	0,62	0,88	0,305	2,0	0,085	2,9	1711	30	1711	33	1721	33	1718	14	1589	46	1578	65	1812	24

34,1	142	106	0,78	0,78	0,38	0,047	2,8	0,018	3,9	286	8	286	8	288	9	292	322	271	21	271	17	515	184
35,1	207	68	0,34	0,34	0,62	0,077	2,8	0,046	9,9	451	13	449	13	453	14	576	426	410	110	374	97	715	220
1.1b	407	236	0,60	0,60	0,30	0,056	1,7	0,041	4,4	307	6	307	6	308	7	293	617	298	42	299	51	398	430
25,1	234	73	0,32	0,32	0,40	0,067	1,7	0,024	7,0	415	7	414	7	414	7	434	69	423	33	418	30	399	50
3.1b	433	355	0,85	0,85	0,24	0,046	2,0	0,013	2,8	284	6	284	6	293	7	294	120	223	10	223	7	1115	46
PANG0001 well																							
1.1p	1218	127	0,11	0,11	2,00	0,065	1,6	0,048	3,9	395	6	395	6	397	6	410	68	295	46	284	35	541	39
2.1p	2025	1705	0,87	0,87	1,14	0,081	1,7	0,067	2,5	373	10	373	7	380	11	353	844	326	68	328	27	881	217
3.1p	1361	308	0,23	0,23	1,10	0,072	1,6	0,086	2,6	401	7	401	6	406	7	391	325	251	105	254	47	785	88
4.1p	1882	1409	0,77	0,77	1,01	0,052	1,6	0,025	4,2	303	5	303	5	305	7	288	375	287	23	288	24	515	263
5.1p	648	271	0,43	0,43	0,64	0,047	2,1	0,027	3,9	279	6	279	6	281	7	277	209	246	26	246	14	547	62
6.1p	1209	1070	0,91	0,91	0,75	0,050	1,6	0,019	2,0	296	5	296	5	304	6	279	178	242	12	243	5	1052	50
1,1	1073	2125	2,04	2,04	0,18	0,088	5,2	0,054	6,3	268	30	267	20	321	50	292	4007	143	88	142	58	2737	1548
2,1	681	405	0,61	0,61	3,31	0,054	3,2	0,044	7,7	275	9	275	11	286	13	264	966	164	43	165	82	1276	418
3,1	843	1024	1,25	1,25	1,23	0,063	1,8	0,045	2,4	268	15	267	5	283	10	277	1968	199	78	199	11	1569	176
4,1	1467	804	0,57	0,57	1,20	0,085	3,3	0,108	5,1	384	14	384	15	380	21	375	889	431	71	433	118	-73	973
5,1	711	111	0,16	0,16	2,57	0,209	1,8	0,079	3,6	1196	20	1196	21	1215	21	1196	45	297	98	296	94	1514	24
6,1	591	610	1,07	1,07	4,44	0,085	4,4	0,042	7,8	440	21	439	20	470	29	464	896	275	64	273	60	1792	330
7.1p	1210	735	0,63	0,63	0,25	0,063	2,3	0,054	9,2	325	8	325	11	326	14	321	961	314	50	314	111	436	847
8.1p	1160	1759	1,57	1,57	0,65	0,102	1,7	0,099	2,4	217	16	213	8	228	20	821	2040	184	69	166	42	1659	1508
9.1p	1267	840	0,68	0,68	9,05	0,063	3,2	0,048	17,0	324	12	324	18	334	23	381	1633	233	72	228	173	1179	933
10.1p	454	402	0,91	0,91	4,04	0,060	1,7	0,023	5,0	347	7	347	7	365	8	339	528	236	33	236	27	1476	189
11.1p	520	262	0,52	0,52	1,80	0,057	2,2	0,050	3,2	305	7	305	7	302	9	311	586	346	48	345	48	-151	550
12.1p	923	772	0,86	0,86	1,22	0,081	1,6	0,038	2,2	459	7	459	7	466	9	458	191	410	21	410	13	892	81
13.1p	1375	1222	0,92	0,92	0,22	0,060	2,2	0,028	2,6	331	8	331	8	349	10	325	487	209	23	210	27	1577	161
14.1p	1127	743	0,68	0,68	3,86	0,068	2,0	0,055	5,3	335	9	335	7	348	11	317	736	213	63	214	43	1313	195

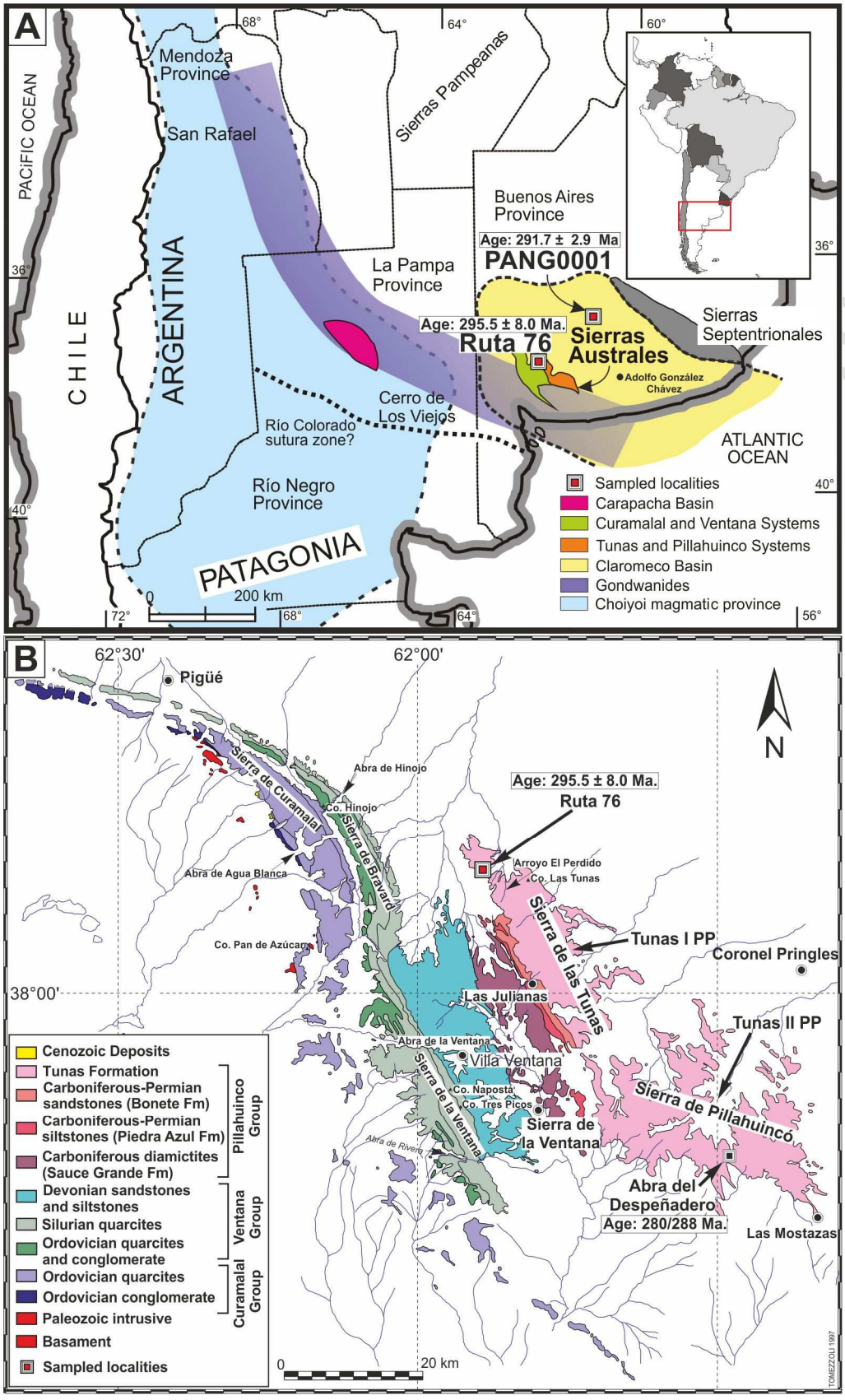
A
Mendoza Province
San Rafael
Sierras Pampeanas
Buenos Aires Province
Age: 291.7 ± 2.9 Ma
PANG0001
La Pampa Province
Age: 295.5 ± 8.0 Ma.
Ruta 76
Sierras Australes
Sierras Septentrionales
Adolfo González Chávez
Cerro de Los Viejos
Río Colorado sutura zone?
ATLANTIC OCEAN
Río Negro Province
PATAGONIA
PACIFIC OCEAN
CHILE
ARGENTINA
200 km
Sampled localities
Carapacha Basin
Curamalal and Ventana Systems
Tunas and Pillahuinco Systems
Claromeco Basin
Gondwanides
Choiyoi magmatic province
B
Pigüé
Sierra de Curamalal
Abra de Hinojo
Co. Hinojo
Sierra de Bravard
Abra de Agua Blanca
Co. Pan de Azúcar
Age: 295.5 ± 8.0 Ma.
Ruta 76
Arroyo El Perdido
Co. Las Tunas
Sierra de las Tunas
Tunas I PP
Coronel Pringles
Las Julianas
Tunas II PP
Abra de la Ventana
Villa Ventana
Sierra de la Ventana
Co. Napostá
Co. Tres Picos
Sierra de la Ventana
Sierra de Pillahuinco
Abra del Despeñadero
Age: 280/288 Ma.
Las Mostazas
N
20 km
Cenozoic Deposits
Tunas Formation
Carboniferous-Permian sandstones (Bonete Fm)
Carboniferous-Permian siltstones (Piedra Azul Fm)
Carboniferous diamictites (Sauce Grande Fm)
Pillahuinco Group
Devonian sandstones and siltstones
Silurian quarcites
Ordovician quarcites and conglomerate
Ordovician quarcites
Ordovician conglomerate
Ventana Group
Curamalal Group
Paleozoic intrusive
Basament
Sampled localities

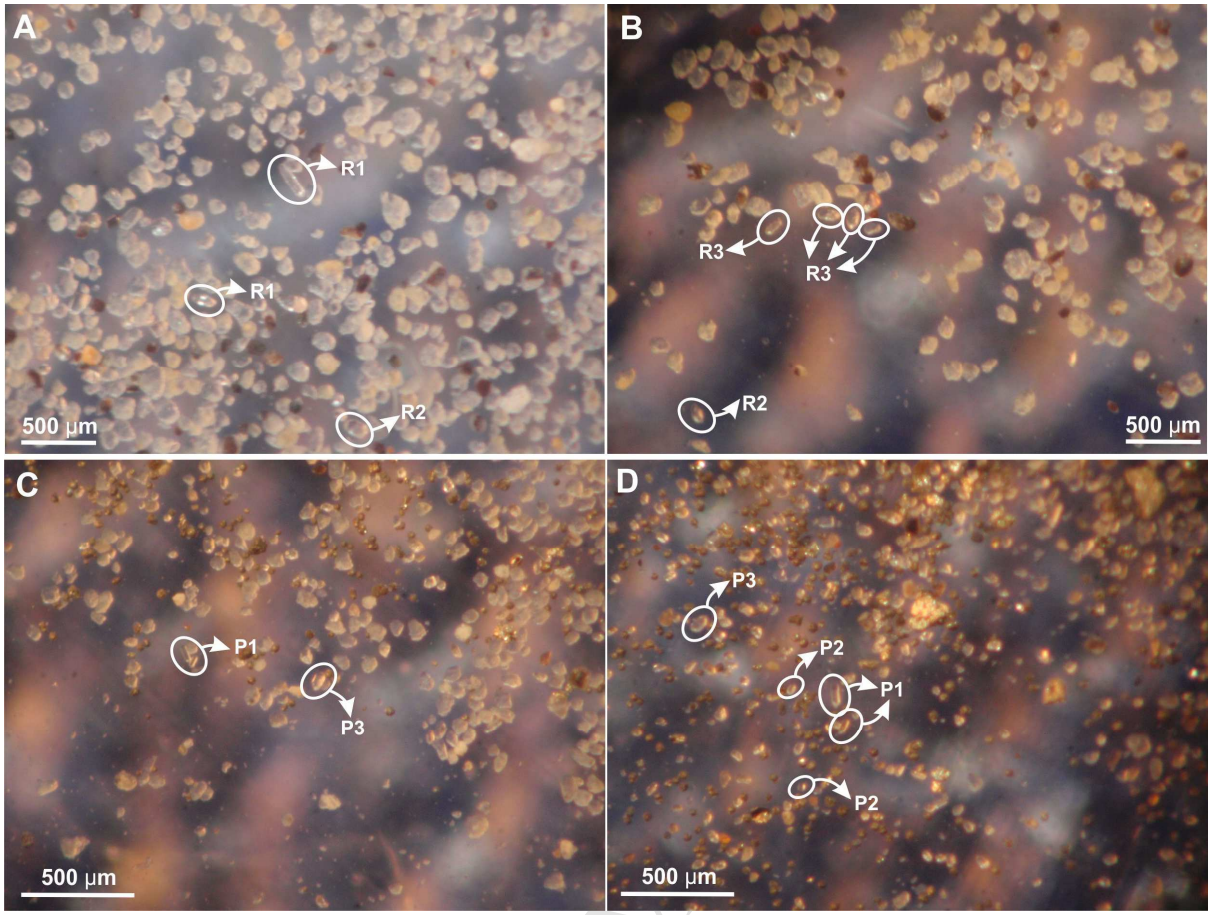

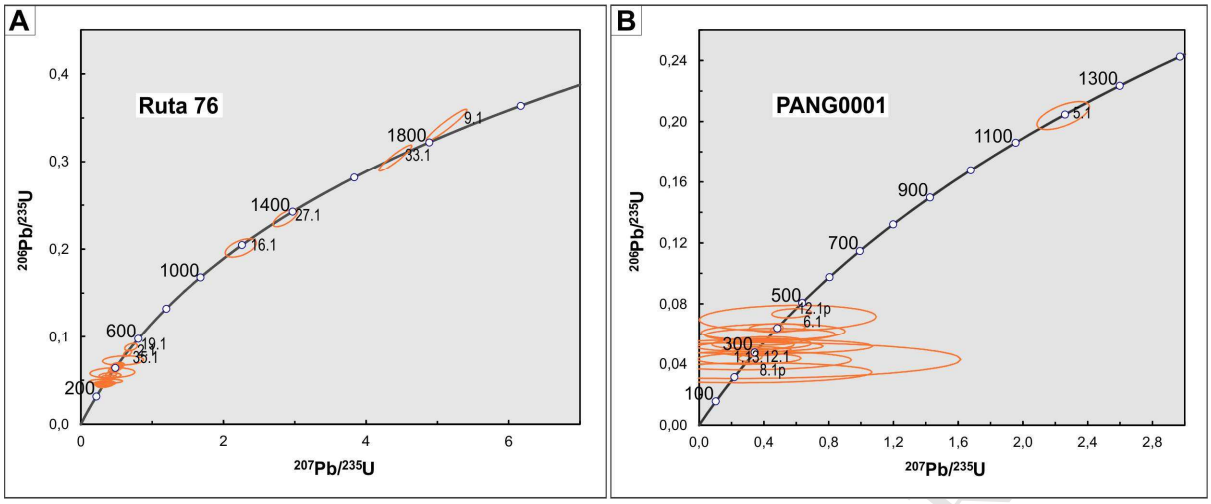

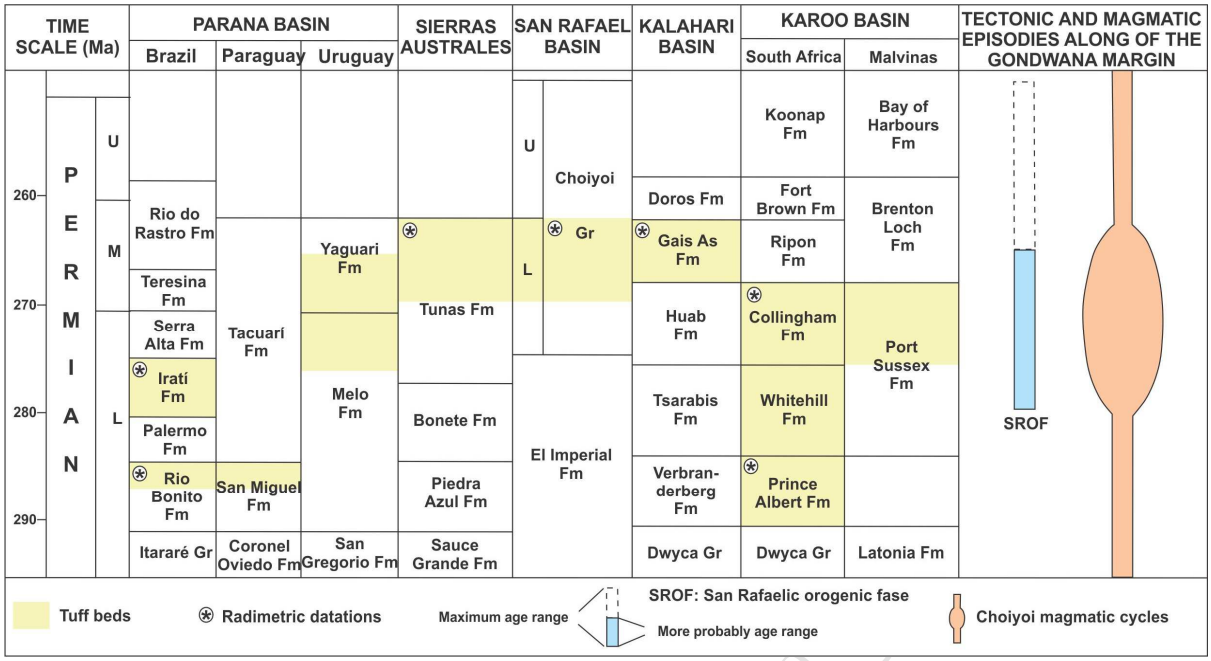

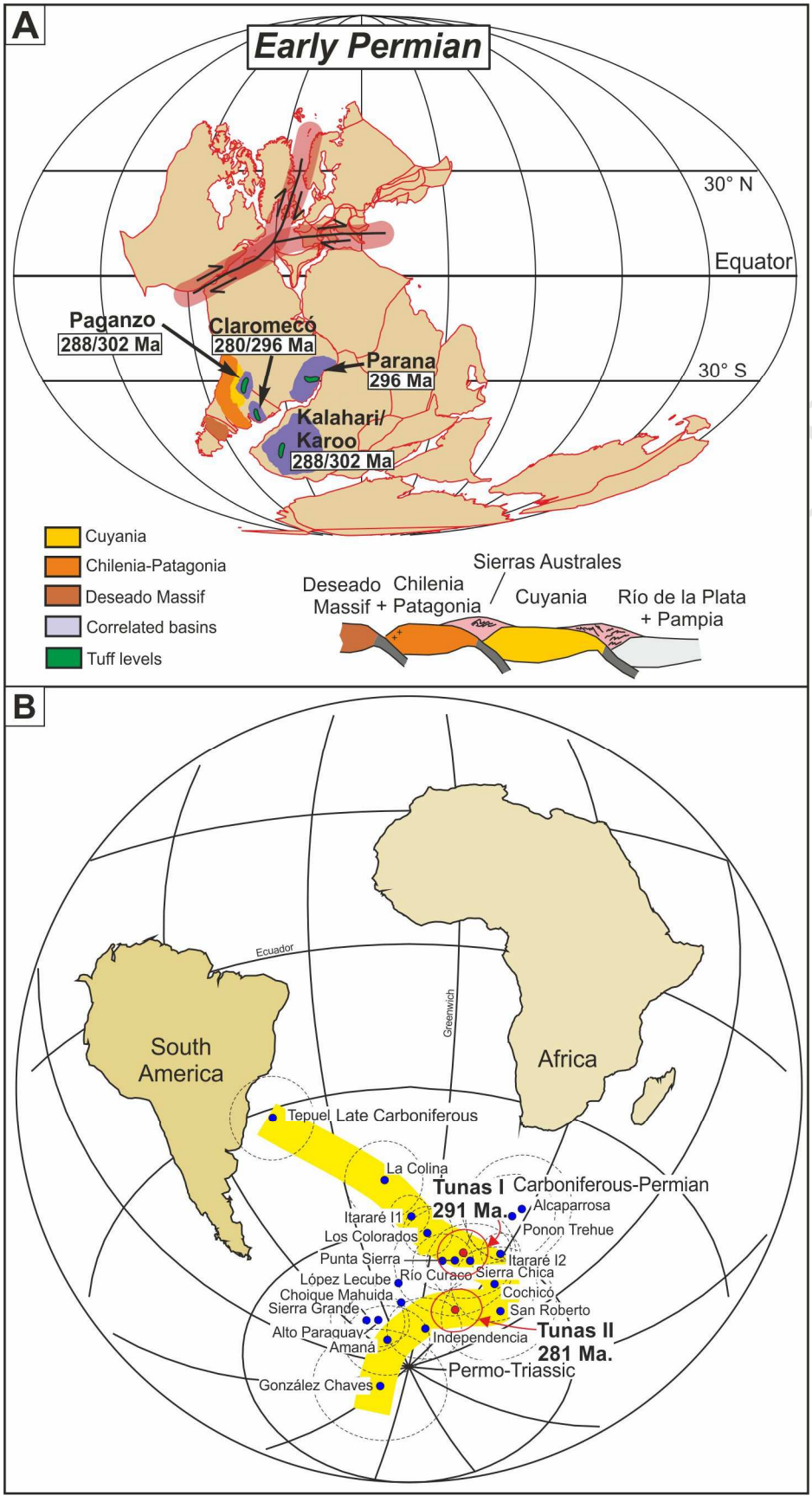
A
Early Permian
30° N
Equator
30° S
Paganzo
288/302 Ma
Claromecó
280/296 Ma
Parana
296 Ma
Kalahari/
Karoo
288/302 Ma
Cuyania
Chilenia-Patagonia
Deseado Massif
Correlated basins
Tuff levels
Sierras Australes
Deseado Massif
Chilenia + Patagonia
Cuyania
Río de la Plata + Pampia
B
Ecuador
Greenwich
South America
Africa
Tepuel Late Carboniferous
La Colina
Tunas I
291 Ma.
Carboniferous-Permian
Alcaparrosa
Itararé I1
Los Colorados
Ponon Trehue
Punta Sierra
Itararé I2
López Lecube
Río Curaco
Sierra Chica
Choique Mahuida
Cochicó
Sierra Grande
San Roberto
Alto Paraguay
Independencia
Tunas II
281 Ma.
Amaná
Permo-Triassic
González Chaves

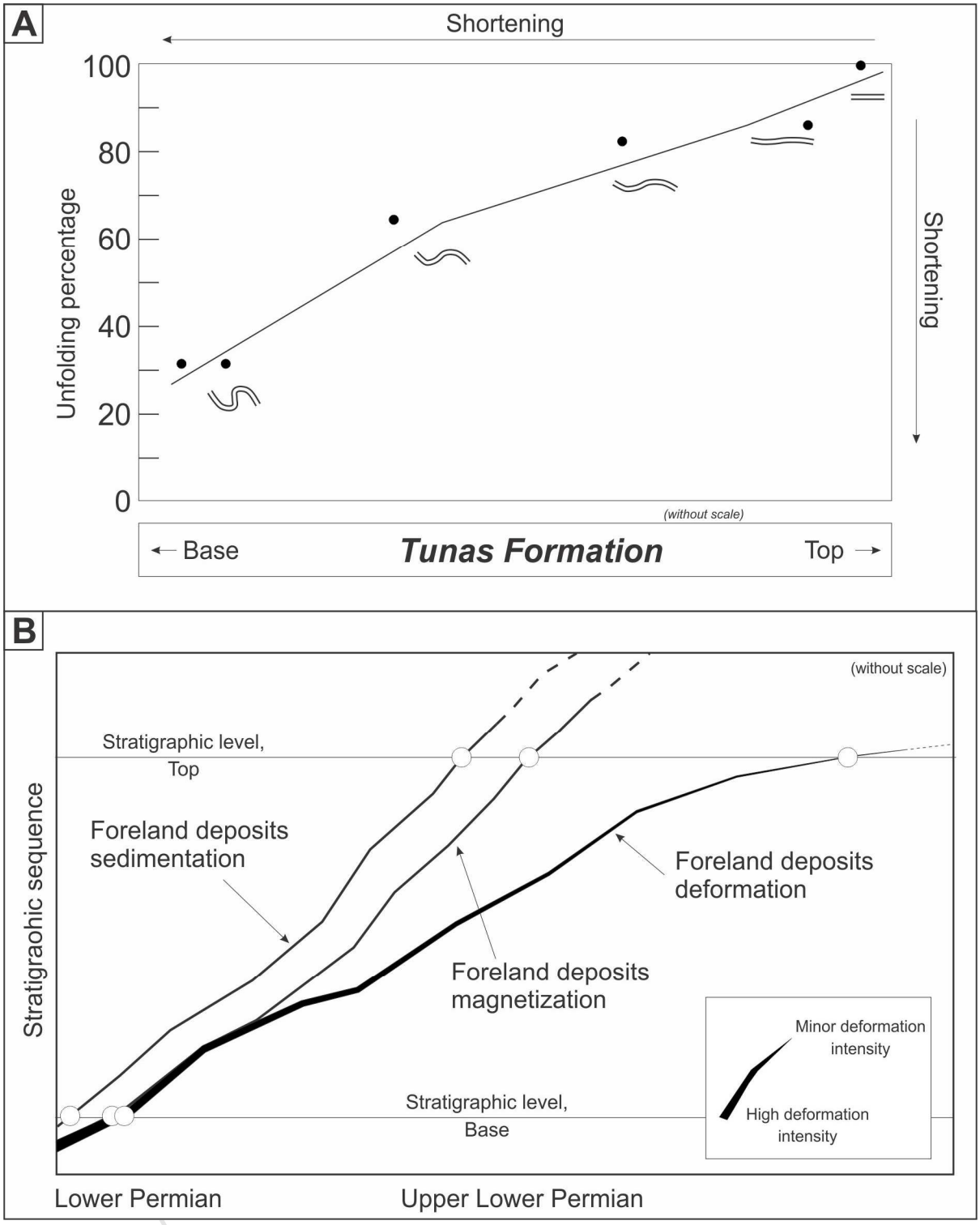
A
Shortening
100
80
60
40
20
0
Unfolding percentage
Shortening
(without scale)
← Base
Tunas Formation
Top →
B
(without scale)
Stratigraphic level,
Top
Foreland deposits
sedimentation
Foreland deposits
deformation
Foreland deposits
magnetization
Minor deformation
intensity
High deformation
intensity
Stratigraphic level,
Base
Stratigraohic sequence
Lower Permian
Upper Lower Permian

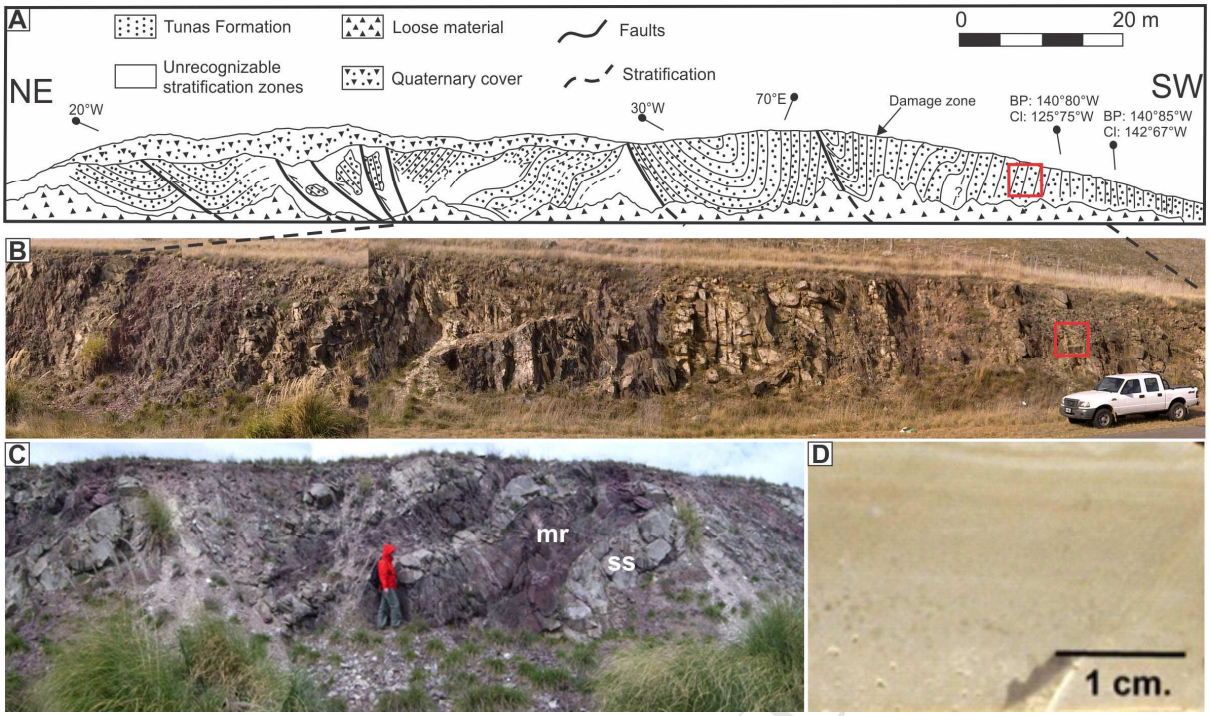

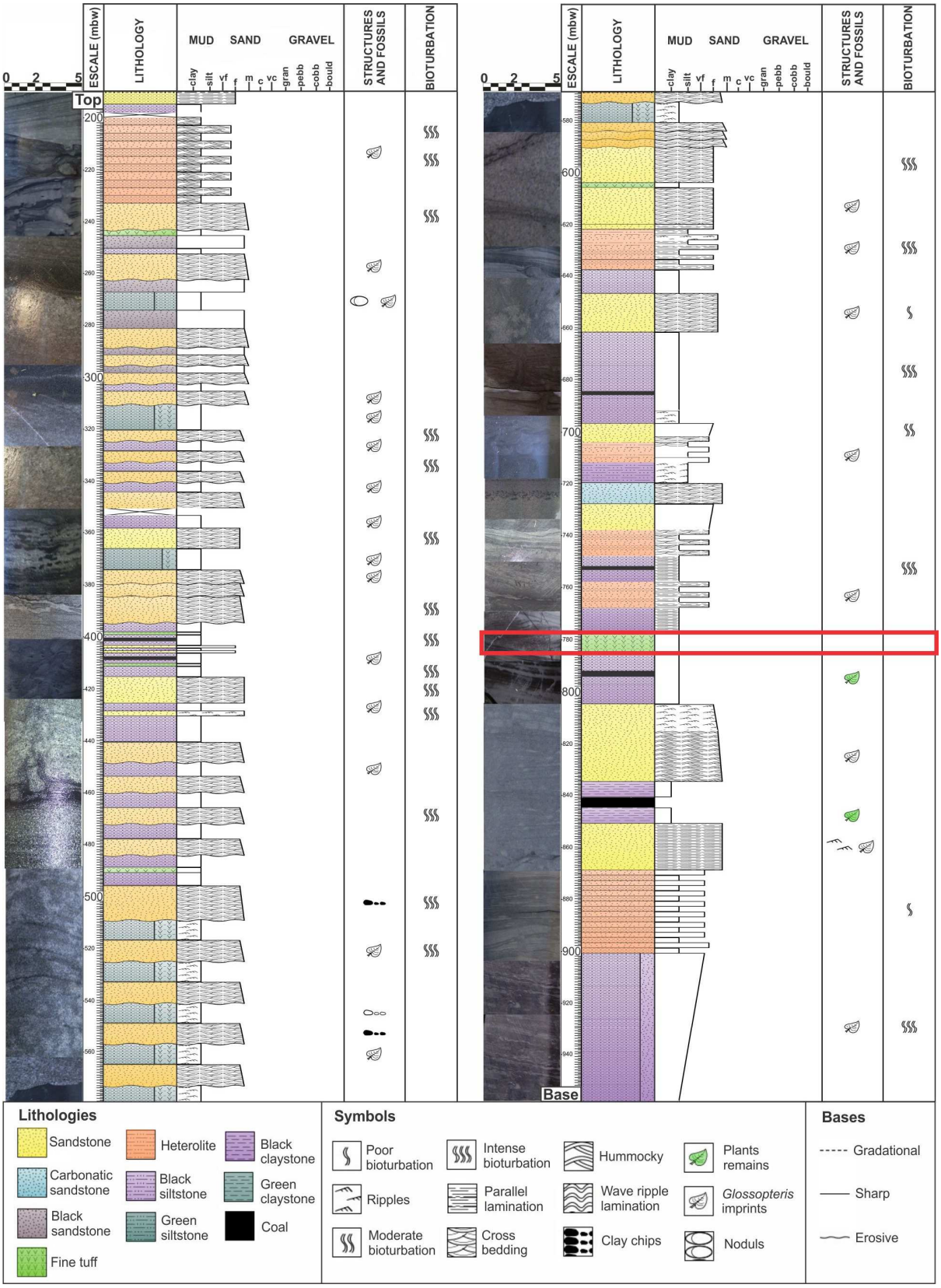
0 2 5
ESCALE (mbw)
LITHOLOGY
MUD SAND GRAVEL
clay silt vf f m c vc gran pebb cobb bould
STRUCTURES AND FOSSILS
BIOTURBATION
Top
Base
Lithologies
Sandstone
Heterolite
Black claystone
Carbonatic sandstone
Black siltstone
Green claystone
Black sandstone
Green siltstone
Coal
Fine tuff
Symbols
Poor bioturbation
Intense bioturbation
Hummocky
Plants remains
Ripples
Parallel lamination
Wave ripple lamination
Glossopteris imprints
Moderate bioturbation
Cross bedding
Clay chips
Noduls
Bases
Gradational
Sharp
Erosive

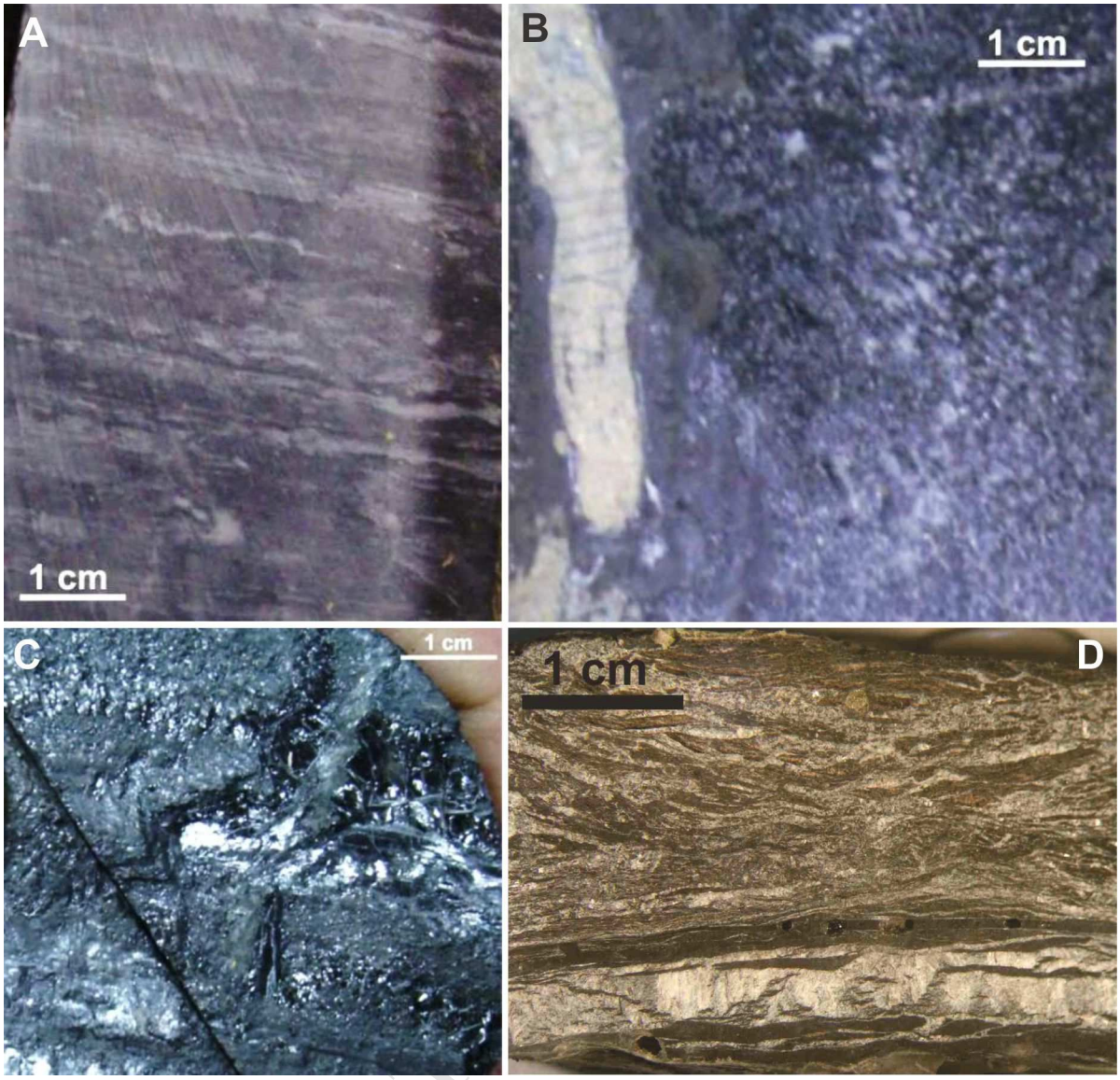

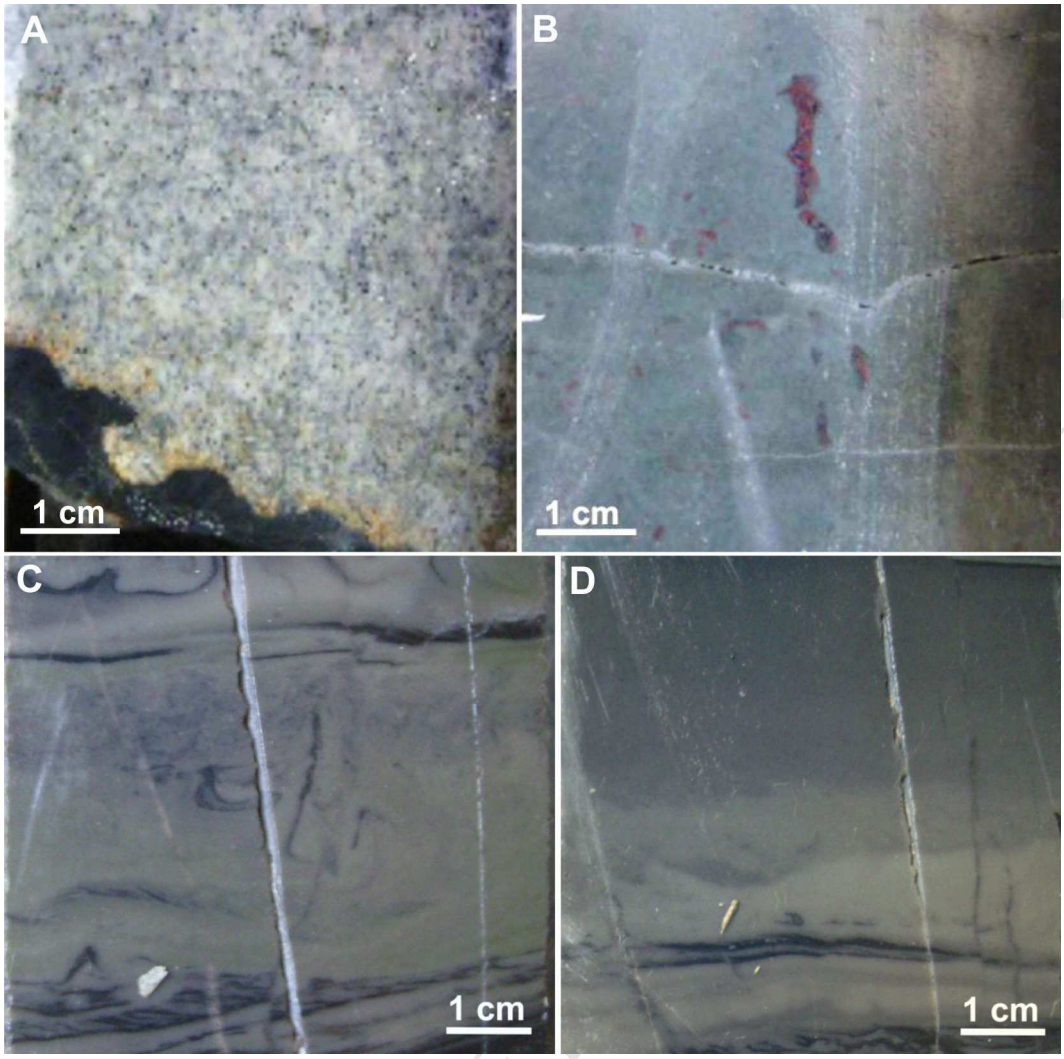

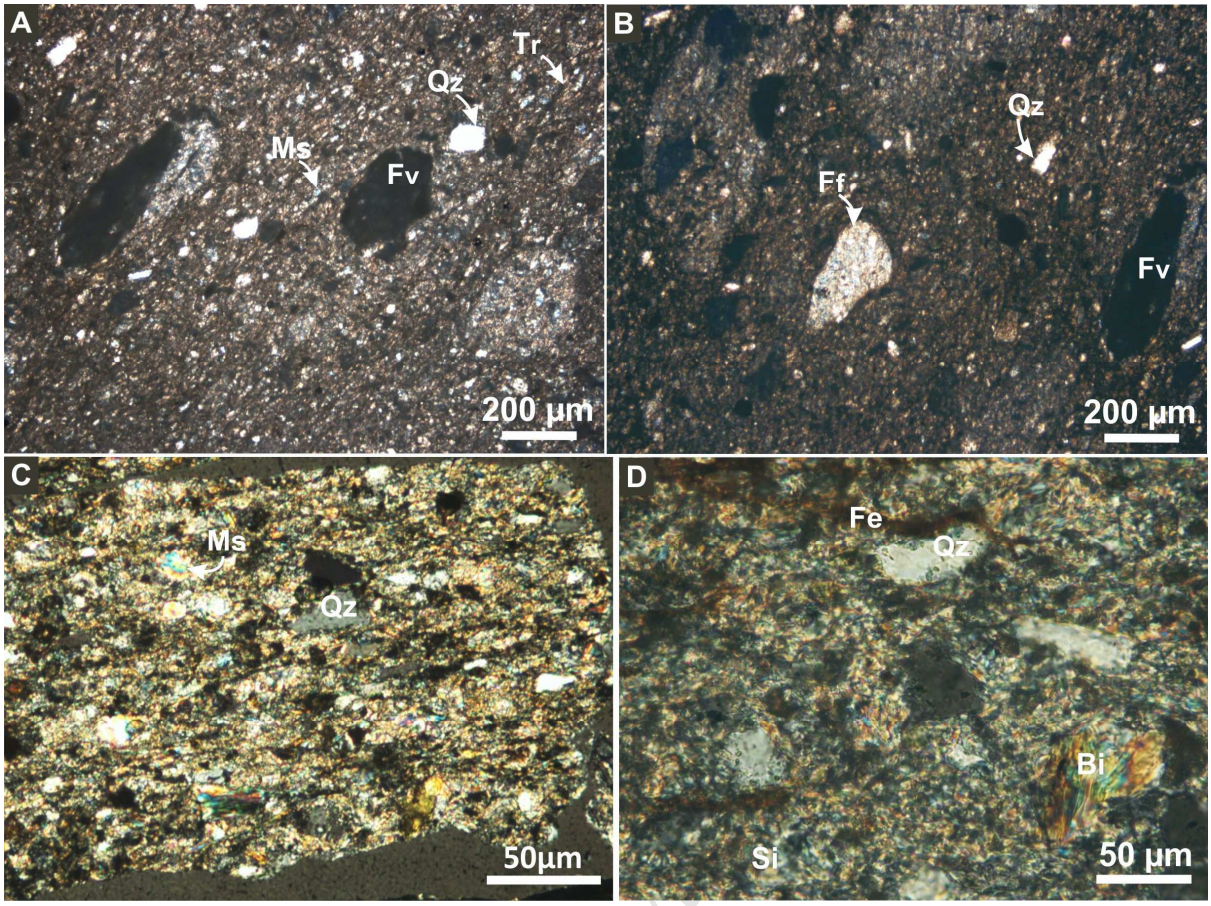

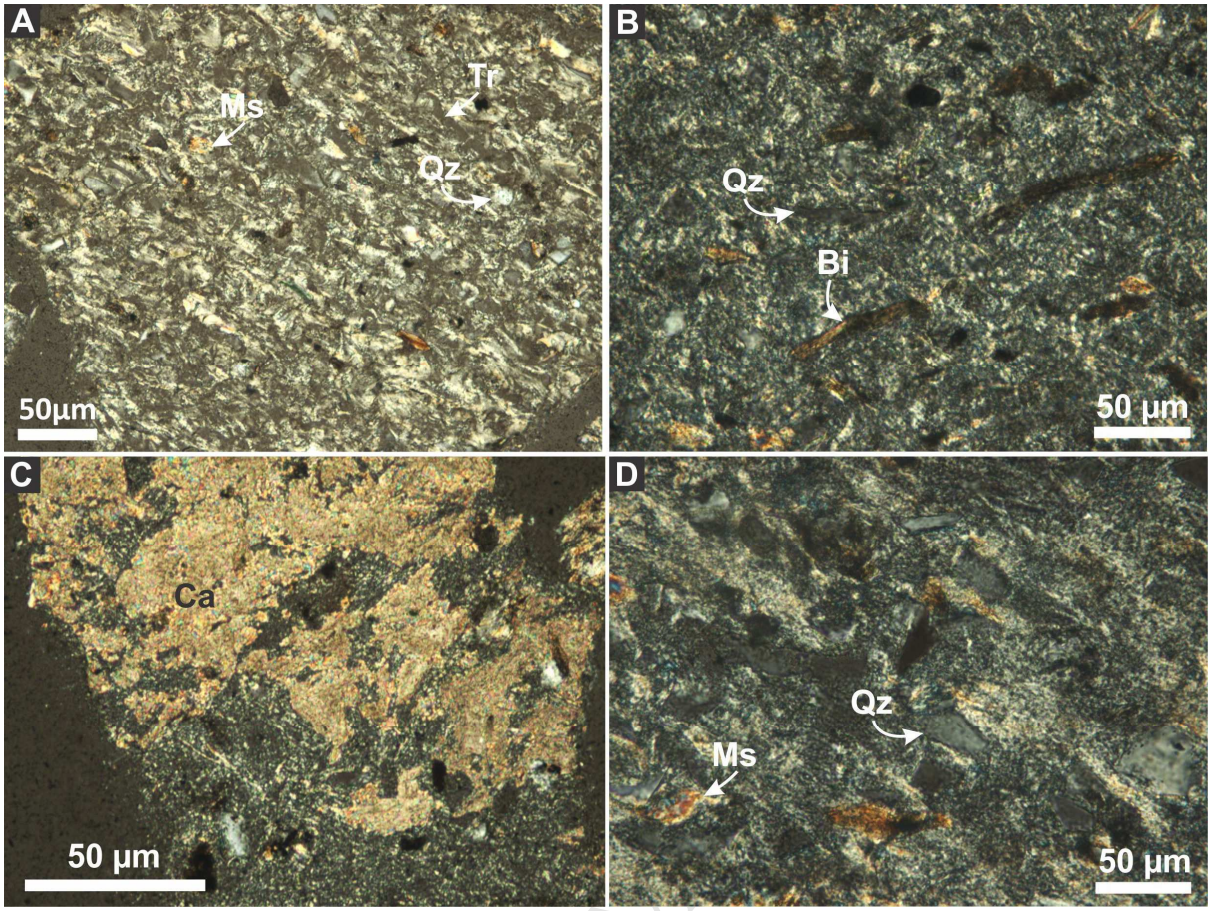

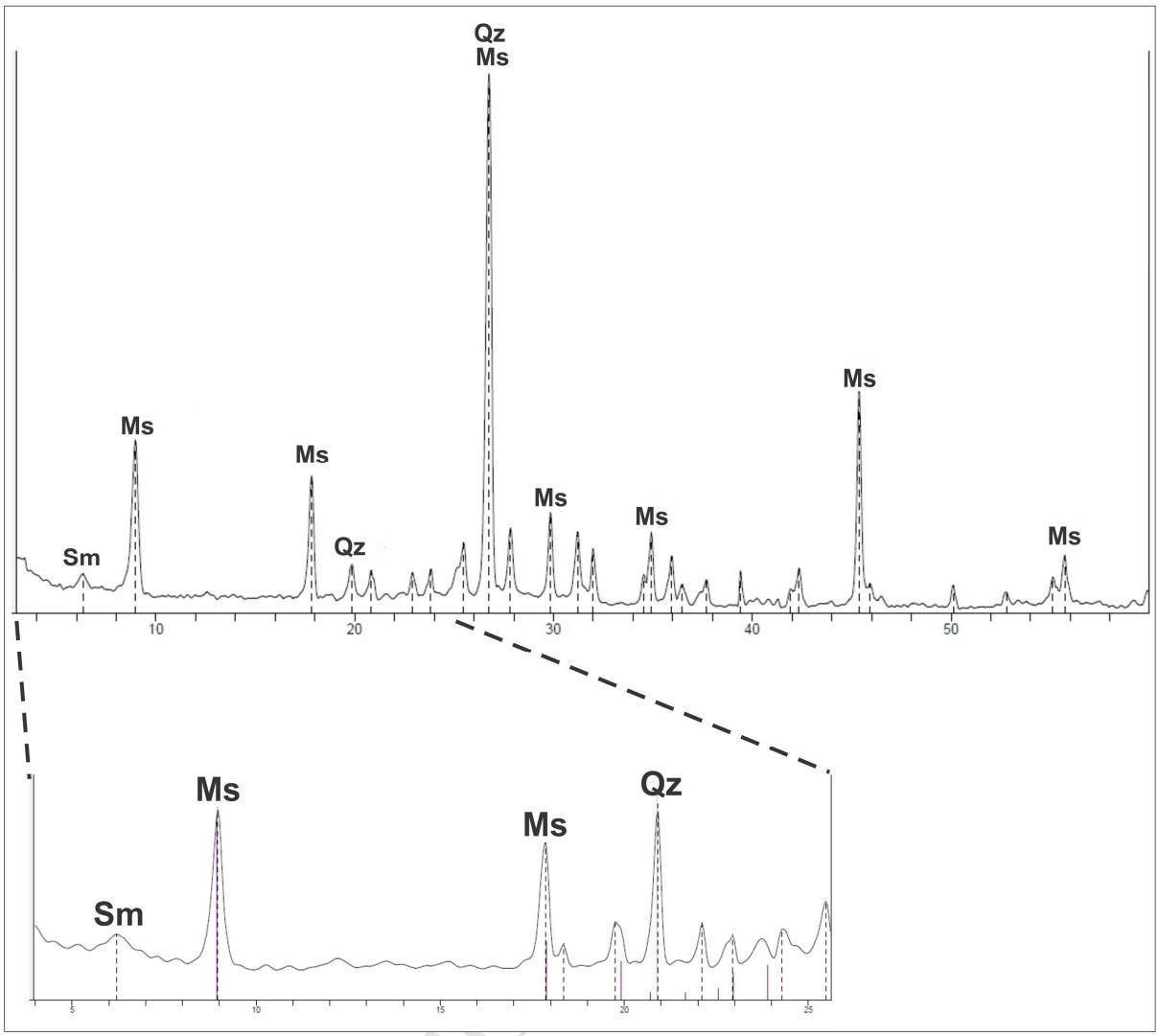

The radimetric ages obtained from SHRIMP analysis in the Tunas Formation, in outcrop and sub-surface tuffs, are 291.7 ± 2.9 and 295.5 ± 8.0 Ma, corresponding to the Early Permian. This age can be assigned to the deposition of the sedimentary sequence and to the coals that are interbedded in it. This new finding would be indicating a synchronous pyroclastic event with the deposition of the Tunas Formation in all its extension.

As the Tunas Formation represent the culmination of the regressive cycle after the carboniferous glaciation, it is also possible to constraint the age of the upper Paleozoic glaciation.

The data, combined with another data, allowed to calculate a northward latitudinal speed of 2.7 cm/year for Gondwana during the Permian and also indicate a tectonically active and changing environment during the Permian of Gondwana. This latitudinal movement would be the consequence of the final coupling of several continental microplates, gradually amalgamated from the southerns margins to Gondwana and from the northern to Laurentia to configurating the Pangea.